Endothelial basement membrane laminins as an environmental cue in monocyte differentiation to macrophages

Lixia Li[*], Jian Song[*], Omar Chuquisana, Melanie-Jane Hannocks, Sophie Loismann, Thomas Vogl[#], Johannes Roth[#], Rupert Hallmann and Lydia Sorokin[§]

Institute of Physiological Chemistry and Pathobiochemistry, Waldeyerstrasse 15;

[#]Institute of Immunology, Röntgenstrasse 21; and Cells-in-Motion Interfaculty Centre, University of Muenster, 48149 Muenster, Germany.

[*]These authors contributed equally to this work.

[§]Corresponding author:

Lydia Sorokin

Institute of Physiological Chemistry and Pathobiochemistry

Muenster University, Waldeyerstrasse 15, 48149 Muenster, Germany

Tel +49 251 8355581; fax +49 251 83 55596; email: sorokin@uni-muenster.de

Summary

Monocyte extravasation is a trigger for differentiation to macrophages. Intravital imaging of CCL2-induced extravasation of CX3CR1-GFP immune cells in mice lacking integral endothelial basement membrane (BM) laminins, *Lama4*$^{-/-}$ and *Tek-cre::Lama5*$^{-/-}$, revealed higher motility of CX3CR1-GFP^{low} inflammatory-monocytes at laminin 511 low sites. *In vitro* experiments revealed that this is not due to direct effects of laminin 511 on migration modes, nor effects on the tightness of the endothelial barrier. Rather, using an intestinal macrophage replenishment model and *in vitro* differentiation studies we demonstrate that endothelial BM laminin 511 uniquely promotes monocyte differentiation to macrophages. This is associated with a change in integrin profile, permitting differentiating macrophages to distinguish between laminin 511 high and low areas and to migrate preferentially across laminin 511 low sites. These studies highlight the endothelial BM as a critical site for monocyte switch to macrophages, and may be relevant to the differentiation of other cells at vascular niches.

Introduction

Monocytes are a diverse population that vary in origin, *in vivo* localization and function. They represent an important early line of defense against infectious agents or reaction to tissue damage and in several tissues, including the intestine, bone marrow derived monocytes play a critical role in the replenishment of resident monocytes, macrophages and dendritic cells (DCs) required for tissue immunity. Trafficking and extravasation are, therefore, critical to their function. Monocytes share similarities with neutrophils in their ability to phagocytose foreign particles and in the molecules employed to extravasate across postcapillary venules (Aurrand-Lions et al., 2005; Woodfin et al., 2011; Woodfin et al., 2007), but show greater heterogeneity in morphology and in the expression of cell surface molecules (Gerhardt and Ley, 2015). There are at least two subsets of monocyte populations, Ly6C^{high}CCR2^{high}CX3CR1^{low} inflammatory monocytes that extravasate into tissues under both sterile and infectious inflammatory conditions, and patrolling monocytes that are Ly6C^{low}CCR2^{low}CX3CR1^{high} (Auffray et al., 2007; Gordon and Taylor, 2005). However, evidence suggests that *in vivo* a continuum of monocyte phenotypes exist that can be modulated by tissue/environmental factors (Dal-Secco et al., 2015). This is illustrated by changes in marker molecule expression only upon monocyte extravasation and include upregulation of MHCII and F4/80 and downregulation of Ly6C (Jakubzick et al., 2013), as well as the recently reported conversion of CCR2^{high}CX3CR1^{low} extravasated cells to CCR2^{low}CX3CR1^{high} cells in inflammatory lesions (Dal-Secco et al., 2015). This

indicates that transendothelial migration of monocytes and subsequent steps are critical for their differentiation to macrophages (Jakubzick et al., 2013).

We have previously shown that the basement membranes (BMs) of vascular endothelium affect extravasation by influencing immune cell migration modes (Sixt et al., 2001a; Wu et al., 2009) and, additionally, by affecting the tightness of endothelial adherens junctions (Song et al., 2017). Specifically, laminin family members were identified as the effector molecules in endothelial BMs, with laminin 511 (composed of α5, β1, γ1 chains) being central to these functions. Endothelial BMs of arteries, arterioles and capillaries typically show high expression of the two main endothelial laminins, laminin 411 and 511, with progressively less laminin 511 occurring in the postcapillary venules, venules and veins, resulting in patches of laminin 411 positive and laminin 511 low expression which define the preferred sites of leukocyte extravasation (Sixt et al., 2001a; Wang et al., 2006b; Wu et al., 2009). Although limited, data suggest that laminin 511 affects T lymphocyte and neutrophil extravasation in different manners; while T cell migration is inhibited by direct interaction with laminin 511 (Wu et al., 2009), neutrophils can migrate across this substrate *in vitro* and their avoidance of laminin 511 high sites *in vivo* rather correlates with the higher endothelial-to-endothelial cell junctional adhesion strength at these sites (Song et al., 2017). Recent intravital imaging of sterile inflammation in the cremaster muscle also revealed that extravasating myeloid cells spend disproportionately long periods of time at the interface between the endothelial monolayer and the endothelial BM and in breaching the BM compared to their rapid penetration of the endothelial monolayer (Song et al.,

2017), suggesting that the subendothelial compartment may be a site of reprogramming required for subsequent steps.

To investigate whether the endothelial BM represents an environmental factor that affects monocyte phenotype or infiltration into tissues, we tracked CX3CR1-GFP monocytes in mice lacking the main endothelial BM laminins, laminin 411 (*Lama4*$^{-/-}$) and laminin 511 (*Tek-cre::Lama5*$^{-/-}$) compared to WT littermates in CCL2-induced extravasation in the cremaster muscle model. As reported for other leukocyte types, extravasation occurred preferentially at laminin 511 low sites; however, *in vitro* experiments revealed that this was not due to direct effects of laminin 511 on migration modes, nor effects on the tightness of the endothelial monolayer. Rather, using an intestinal macrophage replenishment model we demonstrate a novel role for endothelial BM laminin 511 in promoting monocyte differentiation to macrophages, which in turns alters the extent of tissue infiltration. Our data identify the subendothelial space and basement membrane as a site of monocyte switch to macrophages that may also be relevant to other differentiation processes involving cells located at such vascular niches.

Results

Monocyte Extravasation in the Cremaster Muscle Model

To identify extravasating monocytes, bone marrow chimeras were generated by transferring bone marrow cells from CX3CR1$^{GFP/+}$ transgenic mice to *Lama4*$^{-/-}$ and *Tek-cre::Lama5*$^{-/-}$ hosts and their corresponding wild type (WT) littermates. Extravasation was induced by intrascrotal injection of CCL2 and postcapillary venules in the cremaster muscle were intravitally imaged for 4 h or 2 h (Voisin et al., 2009). The number of adherent GFP^{+} monocytes in postcapillary venules were similar in the three chimeras (Fig.1 A, B); however, the extent of extravasation of GFP^{+} monocytes was significantly lower in *Lama4*$^{-/-}$ hosts at 4h compared to WT hosts (Fig. 1 A). At this time point, no differences were measured in extravasated cells between WT and *Tek-cre::Lama5*$^{-/-}$ hosts (Fig. 1A). By contrast, analyses at 2 h after CCL2 application revealed significantly higher numbers of extravasated cells in *Tek-cre::Lama5*$^{-/-}$ hosts (Fig. 1B), indicating that monocytes migrated faster across postcapillary venules that lack laminin α5. Representative images of cremaster muscle venules with extravasated GFP^{+} monocytes are shown in Fig. S1 A, B. This suggests that the absence of laminin α5 in the endothelial BM promotes monocyte extravasation, and its presence as occurs in *Lama4*$^{-/-}$ mice inhibits transmigration as reported for T cells and neutrophils (Song et al., 2017; Wang et al., 2006b; Wu et al., 2009).

To unequivocally identify extravasating cells, tissues were excised following intravital

imaging and examined by confocal microscopy for expression of GFP and MHCII which is only induced upon extravasation (Jakubzick et al., 2013); staining for endothelial BM permitted localization of the monocytes within or outside vessels. This revealed a higher proportion of $GFP^{+}MHCII^{+}$ double positive cells in *Lama4*$^{-/-}$ hosts which, however, remained associated with laminin 511 positive vessels compared to WT controls (Fig. 1C, E) and *Tek-cre::Lama5*$^{-/-}$ hosts (Fig. 1D, F). In *Tek-cre::Lama5*$^{-/-}$ hosts most GFP^{+} were located outside of the vessels and showed minimal MCHII expression (Fig. 1D, F), suggesting that even though more cells extravasated their differentiation towards macrophages was hampered.

Monocyte Accumulation at Laminin $\alpha 5^{high}$ Sites

Using WT hosts carrying CX3CR1-GFP bone marrow we investigated whether a correlation existed between sites of extravasation and laminin 511 expression using fixed tissues collected at 2h after CCL2 administration and analysed by confocal microscopy and *in situ* cytometry. As reported for other leukocytes (Song et al., 2017; Wang et al., 2006b; Wu et al., 2009), extravasating CX3CR1-GFP^{+} cells localized preferentially at laminin $\alpha 5^{low}$ sites (Fig. 2A); however, extensive accumulation of CX3CR1-GFP^{+} cells also occurred within laminin $\alpha 5^{high}$ postcapillary venules (Fig. 2A), which was not observed in TNF-α induced neutrophil extravasation probably because of their faster extravasation compared to monocytes and, hence, absence of accumulation within vessel lumens (Song et al., 2017).

To specifically track CX3CR1-GFP^{low} inflammatory monocytes (Gordon and Taylor, 2005), we analysed GFP mean fluorescence intensity (MFI) in areas of high and low laminin 511 expression using dynamic *in situ* cytometry, confirming a higher proportion of CX3CR1-GFP^{low} cells at laminin 511^{low} than at laminin 511^{high} sites (Fig. 2B, C), and correspondingly higher proportions of CX3CR1-GFP^{high} patrolling monocytes at laminin 511^{high} compared to laminin 511^{low} sites (Fig. 2B, C). Correlation of CX3CR1-GFP MFI with speeds of cell migration, revealed that CX3CR1-GFP^{low} cells had higher average speeds of migration than CX3CR1-GFP^{high} cells (Fig. 2D, E). Similar analyses made at laminin 511 low and high sites revealed higher speeds of migration of cells at laminin 511^{low} sites where extravasation preferentially occurred (Fig. 2F). In *Lama4*$^{-/-}$ hosts, which show a ubiquitous expression of laminin 511 throughout the endothelial BM (Wu et al., 2009) (Fig. 1B), CX3CR1-GFP high and low cells showed comparable migration speeds which were similar to those measured at laminin 511^{high} sites in WT hosts, while CX3CR1-GFP high and low cells showed higher average migration velocities in *Tek-cre::Lama5*$^{-/-}$ hosts (Fig. 2F). Taken together, this suggests that the laminin 511^{low} sites select for the more motile CX3CR1-GFP^{low} inflammatory monocytes, supporting a role for laminin 511 in modulating the phenotype of extravasating monocytes, as suggested above and as we have shown recently for T cells (Zhang et al., 2020).

Mouse monocyte adhesion on laminins *in vitro*

To investigate whether monocytes can bind and distinguish between laminins 411 and 511, *in vitro* adhesion and migration assays were performed. It is not possible to obtain sufficient mouse primary CX3CR1-GFP monocytes for *in vitro* analyses, therefore, mouse monocyte-like Hoxb8 cells (Wang et al., 2006a) and primary human monocytes were employed; control substrates included ICAM-1 and VCAM-1, which are recognized by αLβ2 (LFA-1) and α4β1, respectively. Both human monocytes and mouse Hoxb8 monocytes showed extensive binding to laminin 511, ICAM-1 and VCAM-1, and lower binding to laminin 411 (Fig. 3A, B). However, both cell types also showed high levels of binding to BSA, probably due to activation of integrin β2, which we have previously shown indiscriminately enhances non-specific binding to all substrates including BSA and plastic (Sixt et al., 2001b) (Fig. 3A, B). Mouse integrin β2 null ($CD18^{-/-}$) (Scharffetter-Kochanek et al., 1998) Hoxb8 monocytes or, in the case of human monocytes, anti-human integrin β2 blocking antibody (TS1/18) were, therefore, employed in all subsequent adhesion assays. In both cases, this significantly reduced binding to ICAM-1 and BSA, while the binding to laminin 511 and VCAM-1 remained high, and little or no binding to laminin 411 was measured (Fig. 3A, B).

Flow cytometry revealed similar expression patterns of the main laminin binding integrins on WT and $CD18^{-/-}$ mouse Hoxb8 monocytes and human monocytes, including integrin β1, α6, αv and α5 subunits (Fig. S2A,B) (Kikkawa et al., 2000;

Nishiuchi et al., 2006; Sasaki and Timpl, 2001). To test integrin involvement in binding to laminin 511, function blocking antibodies to integrins $\alpha6$, $\beta1$ or $\beta3$ were employed in adhesion assays. Human monocyte experiments were performed in the presence of anti-integrin $\beta2$ to block non-specific binding and VCAM-1 was employed as a positive control. Blocking integrin $\beta3$ had no effect on the binding of either human monocytes or mouse CD18$^{-/-}$ Hoxb8 monocytes to laminin 511, while blocking integrin $\beta1$ significantly reduced binding to laminin 511 and VCAM-1 (Fig. 3C, D). Inhibition of integrin $\alpha6$ almost eliminated binding of both human and Hoxb8 CD18$^{-/-}$ monocytes to laminin 511 (Fig. 3C, D), suggesting that $\alpha6\beta1$ is the major laminin 511 receptor on mouse and human monocytes (Sasaki and Timpl, 2001).

Monocyte Transmigration Assays

In vitro transwell assays revealed that 25-30% of the human monocytes transmigrated in response to CCL2, surprisingly, with no differences across laminins 411, 511 or BSA or in the presence or absence of anti-integrin $\beta2$ antibody (Fig. 4A). The same pattern of results was obtained with WT and CD18$^{-/-}$ Hoxb8 monocytes in response to C5a (Fig. 4B), indicating that despite differential binding to the laminins, human and murine Hoxb8 monocytes can utilize both substrates for transmigration. We have previously shown similar results using a mixture of splenic monocytes and macrophages (Wu et al., 2009).

We have shown that laminin α5 stabilizes adherens junctions molecules at endothelial junctions, which correlates with reduced transendothelial migration of neutrophils (Song et al., 2017). To address whether this is also the case for monocytes, which may explain the discrepancy between the *in vivo* data and in the *in vitro* transmigration assays, transmigration experiments were performed with human umbilical vein endothelial cells (HUVEC) or mouse b.END5 cells plated at confluent densities on laminins 411, 511 or 111 as a non-endothelial laminin control. Endothelial cells were activated by TNF-α. Both human monocytes and Hoxb8 CD18$^{-/-}$ monocytes showed no differences in the extent of migration across endothelial cells plated on the different laminin isoforms (Fig. 4C, D).

As monocytic cell lines have been reported to express laminin 411 which was proposed to be secreted during extravasation to facilitate penetration of the endothelial BM (Pedraza et al., 2000), we investigated the expression of laminin α4 and α5 polypeptides in cell lysates of naïve and activated mouse Hoxb8 precursors, Hoxb8 monocytes, bone marrow derived macrophages and serum (Fig. S3A, B), and in human monocytes and serum (Fig. S3C,D), revealing the absence of detectable protein in all samples.

Monocyte *in vivo* differentiation

Monocytes and macrophages show different migration capacities on different

substrates (Mercurio and Shaw, 1988; Shaw et al., 1993; Shaw and Mercurio, 1994) and monocytes have been reported to initiate gene expression changes towards a more differentiated MCHII^{+} phenotype upon extravasation (Jakubzick et al., 2013; Thomas-Ecker et al., 2007) which we also observed in *Lama4*$^{-/-}$ mice (Fig. 1C-F). We therefore investigated the possibility of *in vivo* changes in monocyte phenotype during extravasation.

As it is not possible to isolate sufficient leukocytes from the cremaster muscle to phenotype the extravasated GFP^{+} cells, an intestinal model was employed where resident macrophages of the lamina propria (LP) are constantly replenished by circulating monocytes (Zigmond and Jung, 2013). Differentiating monocytes and macrophages, therefore, represent a large fraction of the total LP cells and are well characterized by their differential expression of cell surface markers (Fig. S4A). This permits categorization into early extravasated Ly6C^{high}MHCII^{low} immature P1 and maturing Ly6C^{high}MHCII^{high} P2 populations, and mature Ly6C^{low}MHCII^{high} P3 macrophages (Bain et al., 2014).

Postcapillary venules of the colon wall showed the same the patchy laminin α5 and even laminin α4 distribution as occurs in other tissues (not shown). LP cells from colons of *Lama4*$^{-/-}$ and *Tek-cre::Lama5*$^{-/-}$ mice and WT controls were analysed by flow cytometry using the gating strategy outlined in Fig. S4A at adult stages (3 month-old)

(Fig. 5) and at post-natal day 21 (P21) (Fig. S4B-D), when the peak of colonization of intestinal macrophages by circulating monocytes occurs. In P21 samples, P1 and P2 early extravasating populations were analysed together due to the lower numbers of cells obtained. In both adult and P21 LP, fewer early extravasating P1 and P2 cells were measured in *Lama4*$^{-/-}$ and more in *Tek-cre::Lama5*$^{-/-}$ compared to WT mice (Fig. 5A,B; Fig. S4B,C), reflecting the same pattern of results that were observed in the intravital imaging studies in the cremaster muscle (Fig. 1A, B). However, despite fewer extravasating monocytes, a larger P3 mature macrophage population was measured in *Lama4*$^{-/-}$ LP than in either WT or *Tek-cre::Lama5*$^{-/-}$ LP as reflected by higher P3/P2 ratios (Fig. 5C,D). By contrast, *Tek-cre::Lama5*$^{-/-}$ LP showed lower proportions of P3/P2 ratios than *Lama4*$^{-/-}$ and WT LP (Fig. 5B,C), which was particularly evident in P21 LP (Fig. S4C,D) where a larger proportion of macrophages are derived from infiltrating monocytes (Bain et al., 2014). These results suggest that in the absence of endothelial BM laminin 511, monocyte differentiation to macrophages is reduced and promoted when only laminin 511 is present as occurs in the *Lama4*$^{-/-}$ LP.

Mouse splenic derived monocyte differentiation *in vitro*

As monocyte interaction with vascular endothelial was recently shown to promote differentiation to macrophages in an *in vitro* model (Jakubzick et al., 2013), we tested the role of laminin 511 in this setup. Endothelioma cell lines were generated from *Lama4*$^{-/-}$ and WT littermate embryos (Williams et al., 1989) which expressed high

(eEND4.1) or low (eENDwt) levels of laminin $\alpha5$, respectively (Fig. 6A). However, no endothelioma cell lines from *Tek-cre::Lama5*$^{-/-}$ embryos could be established; similar results were obtained using CRISPR/Cas 9 to eliminate *Lama5* expression in the bEND.5 cell line (manuscript in preparation). Naïve splenic monocytic cells (Fig. S5A, B) were incubated on confluent monolayers of eENDwt or eEND4.1 for 16 h and cells localised at the subendothelial layer were analysed by flow cytometry, revealing a significantly higher proportion of MCHII^{+}Ly6C^{neg} and F4/80^{+}Ly6C^{neg} macrophages in eEND4.1 than in eENDwt cultures (Fig. 6B-E). When the same experiments were performed with splenocytes preincubated in the presence of a function blocking antibody to integrin $\alpha6\beta1$, the proportion of MCHII^{+}Ly6C^{neg} and F4/80^{+}Ly6C^{neg} macrophages in the eEND4.1 cultures were reduced to levels observed in eENDwt cultures (Fig. 6B-E). This substantiates a role for endothelial cell-derived laminin 511 in promoting monocyte differentiation to macrophages, and suggests involvement of both the endothelium and direct, integrin $\alpha6\beta1$-mediated interaction with laminin 511.

Mouse bone marrow derived macrophage (BMDM) migration on laminins

Our data suggest that monocytes only bind significantly to laminin 511 which promotes monocyte differentiate to macrophages. To assess whether differentiation to macrophages alters laminin binding and migratory behavior, WT and CD18$^{-/-}$ BMDM were employed in adhesion assays, revealing the same high integrin $\beta2$-mediated non-specific binding and high specific binding to laminin 511, as observed with monocytes,

but also significant binding to laminin 411 (Fig. 7A). In contrast to Hoxb8 monocytes, BMDM showed slower transmigration in response to C5a with <5% of total cells transmigrating in 4 h, compared to 40% in the case of monocytes. We, therefore, analysed 2D chemotaxis of BMDM using time-lapse video microscopy, revealing $CD18^{-/-}$ BMDM migration on both laminins 411 and 511 but more extensive (Fig. 7B) and faster migration on laminin 411 compared to laminin 511 (Fig. 7C). Similar experiments could not be performed with monocytes as they do not adhere to laminin 411. Flow cytometry of $CD18^{-/-}$ BMDM and monocytes revealed differences in integrin α3, which was expressed on BMDMs but not on human or mouse Hoxb8 monocytes (Fig. S2B, C), and has been reported to bind with high affinity to laminin 511 and laminin 411 (Fujiwara et al., 2001; Kikkawa et al., 2000). $CD18^{-/-}$ BMDMs also expressed slightly higher levels of integrins αv, β3, α6 and α5 compared to monocytes. Unfortunately, a function blocking antibody to mouse integrin α3 does not exist for assessment of its involvement in adhesion to laminin 511 and/or 411. However, integrin $\alpha3\beta1$ has been previously associated with enhanced migratory behavior of leukocytes (Hyun et al., 2012). Hence, even though macrophages migrate more slowly than monocytes, they show altered expression of laminin binding integrins which permits distinction between laminins 411 and 511 and differential migrate on these substrates.

Discussion

It has not been clear to date where the signal for monocytes to switch to macrophage differentiation occurs during extravasation nor the molecular processes involved. While the endothelium has been implicated in this process (Jakubzick et al., 2013), our data demonstrate that it not the endothelium alone but also laminin 511 in the underlying basement membrane that promotes this switch.

Like T cells and neutrophils, CX3CR1-GFP monocytes also preferentially extravasate at laminin 511^{low} sites, with CX3CR1-GFP^{low} inflammatory-monocytes showing preferential localization and higher motility at such sites. However, *in vitro* chemotaxis studies revealed an equal ability of monocytes to migrate across both endothelial laminins and non-endothelial laminins and BSA. While this may reflect shortcomings of the *in vitro* experimental system, we propose that high affinity binding of the infiltrating monocytes to laminin 511 in the endothelial BM traps them at this site and promotes their differentiation towards the macrophage lineage, which alters both their integrin profile and migratory mode. Both monocytes and macrophages bind efficiently to laminin 511 but only macrophages also bind to laminin 411 and can, therefore, distinguish between these two isoforms; they also migrate more efficiently on laminin 411, explaining the faster extravasation of CX3CR1-GFP cells in *Tek-cre::Lama5*$^{-/-}$ hosts. This highlights the site between the endothelial monolayer and the underlying BM as a critical site for the modulation of the phenotype of infiltrating monocytes and

for their switch to macrophages. This is supported by the enhanced macrophage differentiation of splenic monocytes observed in cells cultured together with laminin 511 overexpressing endothelial cell lines and by the higher proportion of differentiating macrophages in the intestines of the *Lama4*$^{-/-}$ mice, which express only laminin 511.

The adhesion of monocytes to endothelium has been reported to trigger expression of extravasation specific genes and to initiate changes towards a more differentiation phenotype (Randolph et al., 1998; Thomas-Ecker et al., 2007). More recently, specifically the site underlying endothelial cells, but not fibroblasts, was shown to be critical for this switch (Jakubzick et al., 2013); however, the molecular basis of these observations remained unclear. Our data suggest that laminin 511 together with the endothelium is critical for this step. The fact that blocking integrin α6 reduced, but did not ablate, the differentiation of monocytes incubated with endothelium overexpressing laminin 511 to macrophages suggests that two steps may be involved – cross-talk with the endothelium, in an as yet undefined manner, and subsequent integrin $\alpha6\beta1$ mediated interaction with laminin 511 in the endothelial BM. The absence of such an effect in monocytes incubated with fibroblasts (8) may be explained by the nature of extracellular matrix that they secrete, which is mainly collagen types I and III and proteoglycans and, in specialized situations, also laminins 411 and 211 (Fleger-Weckmann et al., 2016; Frieser et al., 1997; Schuler and Sorokin, 1995) but not laminin 511 (Sorokin et al., 1997). The relatively long incubation time of monocytes with endothelium required for the *in vitro* differentiation to macrophages (16h), compared

to the time required for monocytes to extravasate into the inflamed cremaster muscle (2-4h), suggests the absence of critical factors in the *in vitro* set up, which may include absence of a mature BM that cannot be recapitulated *in vitro* using cultured cells.

There is increasing evidence that molecularly distinct steps exist subsequent to penetration of the endothelial monolayer that are critical for successful extravasation into inflamed tissues. This is suggested by intravital microscopy studies (Song et al., 2017; Woodfin et al., 2011) and by studies involving blocking of endothelial junctional molecules, such as CD99, CD99L and PECAM-1, that result in leukocyte arrested at cell-cell junctions or at the endothelial BM (Bixel et al., 2004; Liao et al., 1995; Samus et al., 2018; Schenkel et al., 2002; Song et al., 2017). However, the concept that endothelial barrier function and phenotypes of extravasating immune cells may be affected by signals originating from endothelial BM, as suggested here, is only starting to emerge. How BM components affect extravasation is likely to depend on the immune cell and tissue type, e.g. the effects on highly impermeable microvessels of the central nervous system are likely to differ from those on the microvessels of secondary lymphoid organs. Unpublished data from our lab supports a role for endothelial laminins 511 and 411 in modulating the pathogenicity of T cells infiltrating into the brain during neuroinflammation. While the integrins and mechanisms involved are distinct to those described here (Zhang et al., 2020), the data reinforce the sub-endothelial site as important for modulation of immune cell phenotypes during extravasation processes.

We show here that the switch towards a macrophage phenotype is associated with a change in integrin profile, as reported previously by others (Ammon et al., 2000; Prieto et al., 1994; Shaw et al., 1993), with the notable unique expression of integrin $\alpha3\beta1$ by macrophages and increased surface levels of $\alpha v\beta1$, $\alpha6\beta1$, $\alpha5\beta1$ and $\alpha v\beta3$, all of which can bind to laminin 511 and, for $\alpha6\beta1$ and $\alpha3\beta1$, also laminin 411 (Fujiwara et al., 2001; Kikkawa et al., 2000). Such changes are likely to affect the ability of the cells to interact with and to distinguish between the different laminin isoforms. However, differentiation towards the macrophage lineage is also associated with changes in size and cytoplasmic complexity (Jakubzick et al., 2017) that will affect migration potential and speed. The larger size of macrophages (15-20 μm) compared to monocytes (7-8 μm) may contribute to their slower migration across isolated laminins measured here, but the associated larger cytoplasmic volume and more complex cytoskeleton may be an advantage with respect to the force required to penetrate the endothelial BM *in vivo* – topics that require future investigation. Indeed, it may be serendipitous whether an extravasating monocyte encounters a laminin 511 high or low patch in the postcapillary venule BM, which may determine those cells that differentiate towards the macrophage phenotype and those that do not and can re-enter the circulation (Jakubzick et al., 2017), placing endothelial laminin 511 in a pivotal position in the switch from monocytes to macrophages. While we have here examined specifically monocytes/ macrophages, the processes and concepts described may be relevant to other differentiation processes involving cells located at such vascular niches, including stem

cells.

Acknowledgements

We thank Sigmund Budny for purification of laminins, and Barbara Liel for generation of eENDwt and eEND4.1 cells. This work was supported by funding to LS from the German Research Foundation (CRC1009 A02, EXE1003).

Competing Interests

The authors declare no competing interests.

Author contributions

Lixia Li carried out the intravital microscopy (IVM) experiments and most adhesion and migration assays; Jian Song analysed all IVM experiments and carried out all *in vitro* macrophage differentiation experiments; Sophie Loismann performed adhesion assays with WT and CD18$^{-/-}$ Hoxb8 monocytes; Omar Chuquisana performed flow cytometry of Hoxb8 monocytes and BMDM; Thomas Vogl generated WT and CD18$^{-/-}$ Hoxb8 monocyte lines and contributed to writing of the manuscript; Johannes Roth contributed to experimental design and writing of the manuscript; Rupert Hallmann generated and characterised endothelioma cell lines and, together with Melanie-Jane Hannocks, contributed to experimental design, analyses of data and writing of the manuscript; Lydia Sorokin designed the project, supervised all work and wrote the original manuscript.

Figure Legends

Fig. 1 Intravital microscopy of monocyte extravasation in cremaster muscle postcapillary venules of *Lama4*$^{-/-}$ or Tek-cre::*Lama5*$^{-/-}$ hosts carrying CX3CR1$^{GFP/+}$ bone marrow. Adherent and extravasating CX3CR1-GFP^{+} monocytes were quantified at 4 h (A) and 2 h (B) post-application of CCL2. Data are means ± SD from 5 wt mice and 4 mice for each chimera with 4-8 postcapillary venules examined/mouse in (A) and 3-4 wt and chimeric mice with 3-4 postcapillary venules examined/mouse in (B). (C,D) Corresponding excised tissues from A and B were immunofluorescently stained for MCHII and laminin α5 or α4 to identify CX3CR1-GFP^{+}MCHII^{+} extravasating cells in relation to the endothelial basement membrane; scale bar = 50µm. (E, F) Quantification of proportions of CX3CR1-GFP^{+}MCHII^{+} cells expressed as percentage of total GFP^{+} cells in *Lama4* $^{-/-}$ or Tek-cre::*Lama5*$^{-/-}$ hosts. Data are means ± SD from 4 WT and 4 chimeric mice with 2-4 postcapillary venules examined/mouse in (E) and 3 WT and 3 chimeric mice with 3-7 postcapillary venules examined/mouse in (F). Significance in A, B and E and F were calculated using Mann-Whitney tests since not all data passed the normality test by D`Agostino & Pearson; the exact *p*-values are shown in the graph.

Fig. 2 CX3CR1-GFP^{low} inflammatory monocytes preferentially extravasate at laminin 511^{low} sites. (A) Representative confocal microscopy of whole mount cremaster muscle from a WT host carrying CX3CR1$^{GFP/+}$ bone marrow stained with

anti-laminin α5 and anti-PECAM-1 (i); single channel images are shown in (ii, iii, iv); scale bar = 100 μm. Experiment was repeated 3 times with 1 animal with the same results. (B) To track CX3CR1-GFP^{low} inflammatory monocytes GFP mean fluorescence intensity (MFI) was measured *in situ* in areas of high and low laminin 511 expression (marked by boxes in A), revealing a higher proportion of CX3CR1-GFP^{low} cells, expressed as a percent of total GFP^{+} cells, at laminin 511^{low} compared to laminin 511^{high} sites. (C) Quantification of percent CX3CR1-GFP^{low} cells at laminin 511 high and low sites; data are means ± SD of 3 experiments with 1 mouse/experiment with at least 5 sites examined/experiment. (D) Representative plot of the correlation between GFP MFI (Y axis, left, blue line) and the migration speed (Y axis, right, green dots) of 80 individual cells (X-axis) and (E) corresponding quantification of the data from 39 CX3CR1^{hi} and 41 CX3CR1^{low} sites analysed in 3 WT hosts. (F) Average migration velocities of GFP^{+} cells at laminin 511 low and high sites in postcapillary venules of WT, *Lama4*$^{-/-}$ and Tek-cre::*Lama5*$^{-/-}$ hosts. Data are mean values ± SD calculated from 39-64 cells analysed in 3 mice per chimera; movies were captured at 4h post-administration of CCL2. Significance of data in C, E and F were calculated using Mann-Whitney tests since the data did not pass the normality test by D`Agostino & Pearson; the exact *p*-values are shown in the graph.

Fig. 3 Human monocytes and mouse monocyte-like Hoxb8 cells bind differentially to endothelial laminins. Human monocyte (A, C) and mouse monocyte-like Hoxb8 cells (B, D) adhesion to laminins 411, 511, VCAM-1, ICAM-1 or

BSA. To exclude non-specific integrin β2-mediated adhesion, experiments were performed with untreated or integrin β2 antibody (TS1/18) treated human monocytes, and WT and CD18$^{-/-}$ mouse monocyte-like Hoxb8 cell. Adherent cells were counted at 1 h and expressed as number of bound cells/mm^2. (C) Inhibition assays were performed with human monocytes preincubated with TS1/18 and either anti-integrin α6 (GoH3) or β1 (P5D2) antibodies before addition to substrates. (D) Similar experiments were performed with mouse monocyte-like CD18$^{-/-}$ Hoxb8 cells pre-incubated with anti-mouse integrin β1 (Ha2/5), α6 (GoH3) or β3 (2C9.G2) antibodies. Data in C and D are expressed as percent of total cells bound in the absence of blocking antibodies. All data are means ± SD from 4 (B) or 5 (A,C,D) independent experiments with triplicates/experiment. Significance was calculated using a Mann-Whitney test in A, C and D and a Welch`s t-test was applied in B; exact *p*-values are shown in the graph.

Fig. 4 Human monocytes and mouse monocyte-like Hoxb8 cells show no selectivity in migration across laminin substrates. Untreated and TS1/18 treated human monocyte (A) and mouse WT and CD18$^{-/-}$ monocyte-like Hoxb8 (B) cell migration across laminins 411, 511 and BSA coated transwell inserts in response to CCL2 or C5a, respectively. Transmigration of human monocytes (C) and WT monocyte-like Hoxb8 cells (D) across HUVEC or mouse bEND.5 cells plated on laminins 111, 411, or 511 pre-coated transwell inserts. Transmigrated cells were expressed as percentage of total cells added. Data are means ± SD from 3 (B,C,D) or

4 (A) independent experiments with three replicates/experiment/treatment. Significance was calculated using a Mann-Whitney test; exact *p*-values are shown in the graph.

Fig. 5 Monocyte differentiation in colons of *Lama4*$^{-/-}$ and *Tek-cre::Lama5*$^{-/-}$ mice. (A) Representative flow cytometry showing proportions of early extravasating P1 (Ly6C^{hi}MHCII^{low}) and P2 (Ly6C^{mid}MHCII^{mid}) populations, and mature P3 macrophages (Ly6C^{low}MHCII^{hi}) in isolated colonic lamina propria cells from adult WT, *Lama4*$^{-/-}$ and *Tek-cre::Lama5*$^{-/-}$ mice; and (B) corresponding quantification of the data. (C) Ratios of P3 /P2 cells. Data are means ± SD from 3 independent experiments performed with 12 WT, 6 *Lama4*$^{-/-}$ and 6 *Tek-cre::Lama5*$^{-/-}$ mice. Significance was calculated using a Mann-Whitney test; exact *p*-values are shown in the graph.

Fig. 6 Enhanced *in vitro* differentiation of splenic monocytes to macrophages on laminin 511-overexpressing endothelial cells. (A) Western blot for the 400 kDa laminin α5 chain in endothelioma cell lines exhibiting low (eENDwt) and high expression of laminin 511 (eEND4.1). Representative flow cytometry for CD45^{+}F4/80^{+} (B) and CD45^{+}MHCII^{+} (C) in splenic monocytes after 16 h incubation with eEND.wt or eEND4.1 cells in the presence of integrin α6 blocking (GoH3) or isotype control antibody; (D, E) corresponding quantification of the data expressed as a percent of the total CD45^{+} population. Data are means ± SD from 3 experiments with 2

replicates/experiment/treatment. Significance was calculated using a Mann-Whitney test; exact P-values are shown in the graph. Fig. S5 contains flow cytometry of sorted cells employed in B and C before and after 16 h incubation in the absence of endothelial cells.

Fig. 7 Macrophages bind to laminins 511 and 411 and show more efficient 2D migration on laminin 411. (A) Mouse WT and CD18$^{-/-}$ BMDM adhesion to laminins 411, 511, VCAM-1 and ICAM-1. Data are means ± SD of 4 experiments with duplicates/experiment. Significance was calculated using a Mann-Whitney test; exact *p*-values are shown in the graph. (B) Random migration of CD18$^{-/-}$ BMDMs on laminin 411 and laminin 511 were imaged by time-lapse video microscopy; 20 cells on each substrate were tracked and analysed. (C) The velocity of 20 cells on each substrate was measured/ experiment; data shows means ± SD from 1 representative experiment with 20 cells. The experiment was performed 3 times with similar results. Since the data in C passed the normality test by D`Agostino & Pearson it was analysed using a Welch`s t-test. Exact *p*-values are shown in the graph.

Methods

Mice

Wild-type (WT) C57BL/6, laminin α4 knockout mice *(Lama4*$^{-/-}$) (Thyboll et al., 2002), endothelial specific laminin α5 knockout mice (*Tek-cre::Lama5*$^{-/-}$) (Di Russo et al., 2017; Song et al., 2013), and CX3CR1$^{GFP/+}$ mice (Jung et al., 2000) were employed. Equal proportions of male and female mice were employed and no difference were noted between sexes. Animals were held in controlled temperature, humidity and day/night cycles according to the ARRIVE guidelines; female and pre-mating male mice were maintained in groups of a maximum of 5 animals/IIL cage, post-mating males were maintained in separate cages. All animal experiments were performed according to German Animal Welfare guidelines.

Bone marrow chimera generation

Recipient *Lama4*$^{-/-}$ and *Tek-cre::Lama5*$^{-/-}$mice and their corresponding WT littermates were lethally irradiated at 15 Gy. 10^7 bone marrow cells from femurs and tibias of CX3CR1$^{GFP/+}$ mice were intravenously (i.v.) injected into each irradiated mouse. Reconstitution efficiency was analysed at 6 weeks for CD45$^+$GFP$^+$ versus CD45$^+$GFP$^-$ cells, or using the polymorphic lineage determinants (CD45.1 or CD45.2), for tracking GFP$^+$ CD45.1$^+$ donor cells in CD45.2 hosts. Only mice with > 95% donor cell engraftments were employed for intravital microscopic imaging.

Cells

Human umbilical venular endothelial cells (HUVECs) were cultured in endothelial cell growth medium (Promo Cell) at 37°C and 5% CO_2 and used up to passage 5. Endothelioma cell lines were generated from *Lama4*$^{-/-}$ embryos (eEND4.1) and WT littermates (eENDwt) as described previously (Williams et al., 1989); presence or absence of *Lama4* was checked by PCR and laminin α5 protein was quantified by Western blot. All endothelioma cell lines were cultured in DMEM plus 10% fetal calf serum (FCS) at 37°C and 5% CO_2.

Murine Hoxb8 is a myeloid progenitor cell line that can be differentiated to monocytes or macrophages upon removal of β-estradiol (Sigma-Aldrich) (Wang et al., 2006a). Hoxb8 progenitor cell lines were generated from CD18$^{-/-}$ C57BL/6 mice and their WT littermates (Scharffetter-Kochanek et al., 1998) and were cultured in RMPI 1640 containing 10% FCS, 40ng/ml GM-CSF (Promokine) and 1 μM β-estradiol. Differentiation to monocyte-like Hoxb8 cells was induced by removal of β-estradiol from the culture medium for 3 days (Wang et al., 2006a).

Bone marrow was flushed from tibias and femurs of WT C57/BL6 or CD18$^{-/-}$ mice, sieved through a 70 μm sieve and red blood cells lysed in lysis buffer. The cells were pelleted and resuspended in DMEM with 10%FCS. The cells were incubated for 24 h at 37°C and 5% CO_2 on bacterial plates, non-adherent cells were then harvested,

transferred to a new bacterial plate in DMEM plus 10% FCS supplemented with 20 ng/ml M-CSF (Promokine) and cultured for 8 days to generate bone marrow derived macrophages (BMDMs).

Human monocytes were isolated from buffy coats of blood from healthy donors. A two-step procedure with a single gradient in each step was used, which included centrifugation through a Pancoll gradient (Pan-Biotech) (density = 1.070 g/ml) followed by a Percoll (General Electric Company) gradient (density = 1.064 g/ml). Monocyte purity was >85% as defined by flow cytometry for CD14 antibody (M5E2, Biolegend). Monocytes were cultured overnight in McCoy's medium (Sigma-Aldrich) plus 15% FCS at 37°C and 7% CO_2 in Teflon cell culture bags (OriGen) prior to use.

Intravital microscopy

Mice were anesthetized using intra peritoneal (i.p.) injection of a mixture of ketamine hydrochloride (125mg/kg; Sanofi Winthrop Pharmaceuticals) and xylazine (12.5 mg/kg; TranquiVed, Phoenix Scientific) in saline. Intra-scrotal injection of 500 ng CCL2 (Biolegend) in 0.2 ml saline 3.5 h or 1.5 h before cremaster muscle exteriorization was employed to induce monocyte extravasation. Intravital microscopy was performed using an Axioscope A1 microscope equipped with an immersion objective (SW 40/0.75 NA) and stroboscopic epifluorescent illumination (Colibri 2, Zeiss), as described previously (Song et al., 2017). Monocyte extravasation was determined by

quantification of GFP^+ cells in an area extending 75 µm from each side of a vessel over a distance of 100 µm vessel length (representing 1.5 x 10^4 $µm^2$ tissue area). Blood flow center-line velocity was determined by imaging fluorescent beads (0.5µm, Polysciences) injected i.v. before image acquisition, which were converted to mean blood flow velocities by multiplying with an empirical factor of 0.625 (Lipowsky and Zweifach, 1978). Recorded images were analysed using ImageJ software.

To correlate speeds of migration with CX3CR1-GFP expression levels, the ImageJ plugin-TrackMate was used to track the motility of CX3CR1-GFP^{high} and CX3CR1-GFP^{low} cells in laminin 511^{high} and laminin 511^{low} areas; LoG detector was used to detect the CX3CR1-GFP cells and Simple LAP tracker was used for tracking the cells. For speed analyses, at least 60 frames were selected for each track and the mean speed of the track was calculated. Each tracked cell was categorized as CX3CR1-GFP^{high} or CX3CR1-GFP^{low}, based on the initial CX3CR1-GFP^{GFP} fluorescent intensity.

Experiments were performed at least 3 times/chimera. In all experiments 3-9 different postcapillary venules were imaged/ mouse and analysed. Experiments were performed using age and sex matched WT chimera and laminin knockout chimeras. Biological replicates were individual animals/ chimeras, technical replicates were analyses performed on different postcapillary venules in the same animal.

Confocal microscopy

After live cell imaging the cremaster muscle was removed, fixed in 1% PFA for 1h, blocked and permeabilized in PBS containing 5% FCS and 0.5% Triton X-100 for 30 min. Incubations with primary antibodies were performed overnight at 4ºC, followed by secondary antibody incubation for 2 h at room temperature. To quantify the proportions of CX3CR1-GFP+MHCII+ cells in total GFP+ cells, the cremaster muscles were stained by using primary antibodies including rabbit anti-mouse laminin α5 (antibody 405) (Sixt et al., 2001a) or anti-mouse laminin α4 (antibody 377) and Brilliant Violet 411-conjugated rat anti-mouse MHC II (Biolegend); monocytes were identified by CX3CR1^{GFP} expression. Alexa 647- (Dianova) anti-rabbit secondary antibodies were employed. The 2-7 postcapillary venules were imaged/ chimera and the images were analysed using ImageJ software.

Dynamic *in situ* cytometry (Bousso and Moreau, 2012) was employed to investigate associations between laminin 511 expression and CX3CR1-GFP mean fluorescence intensity (MFI): cremaster muscles were stained with rat anti-mouse PECAM-1 (MEC13.3, BD Bioscience) and rabbit anti-mouse laminin α5 (antibody 405) (Sixt et al., 2001a) and monocytes were identified by CX3CR1^{GFP} expression; Alexa 647-conjugated anti-rat and Alexa 555-conjugated anti-rabbit secondary antibodies (Abcam) were employed. CX3CR1-GFP expression was analysed with Flowjo v10.4 and the image files were converted into 'flow cytometry standard' files for analysis by flow cytometry software. Image pixels were reconstituted relative to locations in the X and Y axes; laminin 511^{high} and laminin 511^{low} regions were gated separately and

CX3CR1-GFP MFI were analysed in these two regions. Data were expressed as percent CX3CR1-GFP^{low} cells of total CX3CR1-GFP positive cells in laminin 511^{high} and laminin 511^{low} regions. These analyses were performed on 5 postcapillary venules in each of 3 mice/chimera.

Adhesion assay

Cell attachment assays were performed using dot adhesion assays. 12-well Nunc Maxisorb plates were coated overnight at 4°C with 5 µl dots of 20 µg/ml laminin 411, laminin 511, VCAM-1 (R&D) or ICAM-1 (R&D), wells were blocked with 1% BSA for 1 h at 37 °C and washed with PBS before use. Laminins 411 and 511 were purified as described previously (15). 1 x 10^6 cells in adhesion buffer (DMEM, 0.5% BSA, 50 mM HEPES, pH 7.5) were added to coated wells and allowed to adhere for 1 h at 37°C. Non-adherent cells were removed and attached cells were fixed in 4% paraformaldehyde (PFA) for 10 min and stained by 0.5% crystal violet for 10 min. Cells bound to the dots of different substrates were imaged using an inverse Axiovert microscope (Zeiss) and the number of adherent cells per substrate was quantified using ImageJ software. Adhesion assays were carried out using human monocytes and mouse monocyte-like Hoxb8 cells.

Inhibition assays to assess receptors responsible for adhesion to different substrates involved pre-incubation of cells at 4°C for 30 min prior to addition to protein-coated 12-

well plates with 20 µg/ml anti-human integrin β2 (antibody TS1/18), anti-human integrin β1 (antibody P5D2) and anti-mouse integrin β3 (antibody 2C9.G2), or 50 µg/ml anti-mouse integrin β1 (antibody Ha2/5) and anti-human and mouse integrin α6 (GoH3). Inhibition assays were performed using 20 µg/ml of extracellular matrix protein.

Biological replicates were different batches of Hoxb8 cells or human monocyte preparations used in separate experiments, technical replicates were repetitions of the same test (eg adhesion on a specific laminin isoform) in one experiment.

Migration assays

24-well Transwell inserts (6.5 mm^2) with polycarbonate filters (5 µm pore size) (Corning Costar) were used for transmigration assays. Membranes were coated overnight at 4 °C with 10 µg/ml laminins 411 or 511 and blocked with 1% BSA in PBS for 1 h at 37°C. Human monocytes, mouse Hoxb8 monocytes and BMDM were used in transmigration assays. 5 x 10^5 cells in 100 µl adhesion buffer were added to the upper chamber and either 500 ng/ml CCL2 (R&D Systems) or 10 nM C5a (R&D Systems) was added to the bottom chamber. Cells were permitted to transmigrate at 37°C for 4h, and the number of transmigrated cells was expressed as a percentage of the total cells initially added. For trans-endothelial migration, HUVEC or bEND.5 cells were plated at confluent densities onto the laminin 411, 511 or 111 coated filters and stimulated for 4 h with 5nM tumor necrosis factor-α (TNF-α; R&D Systems), then human monocytes or monocyte Hoxb8 cells were added. These experiments were 3

times with triplicates/ experiment.

2D Chemotaxis assays utilized the Ibidi μ-Slide Chemotaxis system and 20nm C5a as chemoattractant. Slides were coated overnight at 4°C with 10 μg/ml laminin 411 or 511, and mouse WT or CD18$^{-/-}$ lipopolysaccharide (LPS/1 μg/ml) (Sigma) activated BMDM cells (1x10^{6} cells/ml) were added in attachment buffer (RPMI 1640 medium, 20 mM Hepes, 10 % FCS) and monitored by time-lapse video microscopy every 2 min for 24h. Cell migration tracks between 6-12 h were analysed by ImageJ using a manual tracking plugin and the Ibidi software chemotaxis and migration tool. A minimum of 20 randomly selected cells on each substrate were manually tracked and cell velocities were measured/ experiment. The experiment was repeated 3 times.

Isolation of colonic lamina propria (LP) cells

LP cells were purified from colons of adult (8-12 week-old) and day 21 postnatal (P21) mice by enzymatic digestion (Bain et al., 2014). Colons were excised and washed in PBS, opened longitudinally and cut into 0.5 cm sections, and shaken vigorously in Hank's balanced salt solution (HBSS) containing 2% FCS. To remove the epithelial layer, 2 mM EDTA in Ca^{2+}/Mg^{2+} free HBSS was added twice with shaking for 15 min each at 37°C. The remaining tissue was incubated in digestion buffer (RPMI 1640, 10% FCS, 1.25 mg/ml collagenase D (Roche), 0.85 mg/ml collagenase V (Sigma–Aldrich),

1 mg Dispase (Gibco), and 30 U/ml DNase (Roche)) for 30–45 min at 37°C with shaking. The resulting cell suspension was passed through a 40 µm cell strainer and washed twice in RPMI 1640. The experiments for adult and P21 mice were done 3 times with at least 2 mice/mouse strain/experiment. Typically, 4-5 million single cells were obtained from 1 adult colon, and approximately 2 million single cells from one P21. Total numbers of cells isolated in adult or P21 colons were the same regardless of geneotype.

Flow cytometry

Colonic LP samples (2 million cell/staining) were stained at 4°C for 20 min with the following antibodies: Ly6C-FITC (AL-21, BD Pharmingen), F4/80-PE (BM8, BioLegend), Siglec F-PE-CF594 (E50-2440, BD Bioscience), Ly6G PE-Cy7 (1A8, BioLegend), CD11b-APC (M1/70, eBioscience), CD11c-AF700 or -APC-R700 (N418, BioLegend), MHCII-BV421 (M5/114.15.2, BioLegend), and CD45-BV510 (30-F11, BioLegend)) at 4°C for 20 min (Bain et al., 2014). Dead cells were identified by staining with eFluor 780 Fixable Viability dye (eBioscience) and gatings were performed as described previously (Bain et al., 2014).

For analyses of integrin receptors on human monocytes, mouse Hoxb8 monocytes and mouse BMDMs, antibodies to integrins β1 (mouse 9EG7 (Lenter et al., 1993)/

human P5D5) (Wayner et al., 1988), α6 (GoH3, BD Pharmingen), α5 (mouse 5H10-27, BD Pharmingen / human P1D6) (Wayner et al., 1988), α4 (PS/2, Abcam), α3 (mouse polyclonal, R&D/ human P1B5) (Wayner et al., 1988), β3 (mouse 2C9.G2, Biolegend/ human B3A, Chemicon) and huan β2 (mouse C71/16, BD Pharmingen / human TS1/18, Thermo Scientific) were employed. Cells were analysed with a Gallios (Beckman Coulter) or Celesta (BD) flow cytometer and FlowJo software.

***In vitro* monocyte differentiation**

3D Collagen type I was prepared using 8 parts rat collagen type I (Sigma) and 1 part 10x DMEM and was neutralized to pH 7.0-7.5 by adding 0.5 parts 0.5N NaOH; 400 µl collagen I gel was then added immediately to each well of a 24-well plate. Endothelial cells (e.END4.1, e.ENDwt) were seeded onto the collagen type I gel base and were incubated at 37°C overnight. Splenic monocytes were isolated by depleting CD19, Ly6G, CD11c, CD3ε, Siglec-F, MHCII and CD11C positive cells using magnetic beads (Miltenyi Biotec); 5 x10^5 cells were plated onto the confluent endothelial cells for 16 h at 37°C. Unattached cells were removed by 5x washing with DMEM; 400 µl Collagenase D (2 mg/ml, Sigma) was then added and the cultures digested at 37°C for 30 min. Cells were harvested and analysed by flow cytometry for PECAM-1, Ly6C, MHCII, CD11b and F4/80 expression. The same experiments were performed with splenocytes preincubated for 30 min in the presence of 25 µg /ml integrin α6 function blocking antibody (GoH3) or an isotype control. Experiments were performed 3 times

using cells from 2 mice.

Statistical analyses

Data sets were tested for normal distribution with a D`Agostino & Pearson normality test. If all data sets of one experiment passed the normality test, significance was analysed with a Welch`s t-test. A Mann-Whitney test was applied if the data was not normally distributed. P-values of <0.05 were considered significant.

References

Ammon, C., S.P. Meyer, L. Schwarzfischer, S.W. Krause, R. Andreesen, and M. Kreutz. (2000). Comparative analysis of integrin expression on monocyte-derived macrophages and monocyte-derived dendritic cells. Immunology. *100*,364-369.

Auffray, C., D. Fogg, M. Garfa, G. Elain, O. Join-Lambert, S. Kayal, S. Sarnacki, A. Cumano, G. Lauvau, and F. Geissmann. (2007). Monitoring of blood vessels and tissues by a population of monocytes with patrolling behavior. Science. *317*,666-670.

Aurrand-Lions, M., C. Lamagna, J.P. Dangerfield, S. Wang, P. Herrera, S. Nourshargh, and B.A. Imhof. (2005). Junctional adhesion molecule-C regulates the early influx of leukocytes into tissues during inflammation. J Immunol. *174*,6406-6415.

Bain, C.C., A. Bravo-Blas, C.L. Scott, E.G. Perdiguero, F. Geissmann, S. Henri, B. Malissen, L.C. Osborne, D. Artis, and A.M. Mowat. (2014). Constant replenishment from circulating monocytes maintains the macrophage pool in the intestine of adult mice. Nat Immunol. *15*,929-937.

Bixel, G., S. Kloep, S. Butz, B. Petri, B. Engelhardt, and D. Vestweber. (2004). Mouse CD99 participates in T-cell recruitment into inflamed skin. Blood. *104*,3205-3213.

Bousso, P., and H.D. Moreau. (2012). Functional immunoimaging: the revolution continues. Nat. Rev. Immunol. *12*,858-864.

Dal-Secco, D., J. Wang, Z. Zeng, E. Kolaczkowska, C.H. Wong, B. Petri, R.M. Ransohoff, I.F. Charo, C.N. Jenne, and P. Kubes. (2015). A dynamic spectrum of monocytes arising from the in situ reprogramming of CCR2+ monocytes at a site of sterile injury. J Exp Med. *212*,447-456.

Di Russo, J., A.L. Luik, L. Yousif, S. Budny, H. Oberleithner, V. Hofschroer, J. Klingauf, E. van Bavel, E.N. Bakker, P. Hellstrand, A. Bhattachariya, S. Albinsson, F. Pincet, R. Hallmann, and L.M. Sorokin. (2017). Endothelial basement membrane laminin 511 is essential for shear stress response. EMBO J. *36*,183-201.

Fleger-Weckmann, A., Y. Ustun, J. Kloepper, R. Paus, W. Bloch, Z.L. Chen, J. Wegner, L. Sorokin, L. Langbein, B. Eckes, P. Zigrino, T. Krieg, and R. Nischt. (2016). Deletion of the epidermis derived laminin gamma1 chain leads to defects in the regulation of late hair morphogenesis. Matrix Biol. *56*,42-56.

Frieser, M., H. Nockel, F. Pausch, C. Roder, A. Hahn, R. Deutzmann, and L.M. Sorokin. (1997). Cloning of the mouse laminin alpha 4 cDNA. Expression in a subset of endothelium. Eur J Biochem. *246*,727-735.

Fujiwara, H., Y. Kikkawa, N. Sanzen, and K. Sekiguchi. (2001). Purification and characterization of human laminin-8. Laminin-8 stimulates cell adhesion and migration through alpha3beta1 and alpha6beta1 integrins. J Biol Chem. *276*,17550-17558.

Gerhardt, T., and K. Ley. (2015). Monocyte trafficking across the vessel wall. Cardiovasc Res. *107*,321-330.

Gordon, S., and P.R. Taylor. (2005). Monocyte and macrophage heterogeneity. Nat. Rev. Immunol. *5*,953-964.

Hyun, Y.M., R. Sumagin, P.P. Sarangi, E. Lomakina, M.G. Overstreet, C.M. Baker, D.J. Fowell, R.E. Waugh, I.H. Sarelius, and M. Kim. (2012). Uropod elongation is a common final step in leukocyte extravasation through inflamed vessels. J Exp Med. *209*,1349-1362.

Jakubzick, C., E.L. Gautier, S.L. Gibbings, D.K. Sojka, A. Schlitzer, T.E. Johnson, S. Ivanov, Q. Duan, S. Bala, T. Condon, N. van Rooijen, J.R. Grainger, Y. Belkaid, A. Ma'ayan, D.W. Riches, W.M. Yokoyama, F. Ginhoux, P.M. Henson, and G.J. Randolph. (2013). Minimal differentiation of classical monocytes as they survey steady-state tissues and transport antigen to lymph nodes. Immunity. *39*,599-610.

Jakubzick, C.V., G.J. Randolph, and P.M. Henson. (2017). Monocyte differentiation and antigen-presenting functions. Nat. Rev. Immunol. *17*,349-362.

Jung, S., J. Aliberti, P. Graemmel, M.J. Sunshine, G.W. Kreutzberg, A. Sher, and D.R. Littman. (2000). Analysis of fractalkine receptor CX(3)CR1 function by targeted deletion and green fluorescent protein reporter gene insertion. Mol. Cell. Biol. *20*,4106-4114.

Kikkawa, Y., N. Sanzen, H. Fujiwara, A. Sonnenberg, and K. Sekiguchi. (2000). Integrin binding specificity of laminin-10/11: laminin-10/11 are recognized by alpha 3 beta 1, alpha 6 beta 1 and alpha 6 beta 4 integrins. J Cell Sci. *113 (Pt 5)*,869-876.

Korpos, E., N. Kadri, R. Kappelhoff, J. Wegner, C.M. Overall, E. Weber, D. Holmberg, S. Cardell, and L. Sorokin. (2013). The peri-islet basement membrane, a barrier to infiltrating leukocytes in type 1 diabetes in mouse and human. Diabetes. *62*,531-542.

Lenter, M., H. Uhlig, A. Hamann, P. Jeno, B. Imhof, and D. Vestweber. (1993). A monoclonal antibody against an activation epitope on mouse integrin chain beta 1 blocks adhesion of lymphocytes to the endothelial integrin alpha 6 beta 1. Proc. Natl. Acad. Sci. USA. *90*,9051-9055.

Liao, F., H.K. Huynh, A. Eiroa, T. Greene, E. Polizzi, and W.A. Muller. (1995). Migration of monocytes across endothelium and passage through extracellular matrix involve separate molecular domains of PECAM-1. J Exp Med. *182*,1337-1343.

Lipowsky, H.H., and B.W. Zweifach. (1978). Application of the "two-slit" photometric technique to the measurement of microvascular volumetric flow rates. Microvasc. Res. *15*,93-101.

Mercurio, A.M., and L.M. Shaw. (1988). Macrophage interactions with laminin: PMA selectively induces the adherence and spreading of mouse macrophages on a laminin substratum. J Cell Biol. *107*,1873-1880.

Nishiuchi, R., J. Takagi, M. Hayashi, H. Ido, Y. Yagi, N. Sanzen, T. Tsuji, M. Yamada, and K. Sekiguchi. (2006). Ligand-binding specificities of laminin-binding integrins: a comprehensive survey of laminin-integrin interactions using recombinant alpha3beta1, alpha6beta1, alpha7beta1 and alpha6beta4 integrins. Matrix Biol. *25*,189-197.

Pedraza, C., T. Geberhiwot, S. Ingerpuu, D. Assefa, Z. Wondimu, J. Kortesmaa, K. Tryggvason, I. Virtanen, and M. Patarroyo. (2000). Monocytic cells synthesize, adhere to, and migrate on laminin 8. J. Immunol. *165*,5831-5838.

Prieto, J., A. Eklund, and M. Patarroyo. (1994). Regulated expression of integrins and

other adhesion molecules during differentiation of monocytes into macrophages. Cell. Immunol. *156*,191-211.

Randolph, G.J., S. Beaulieu, S. Lebecque, R.M. Steinman, and W.A. Muller. (1998). Differentiation of monocytes into dendritic cells in a model of transendothelial trafficking. Science. *282*,480-483.

Ringelmann, B., C. Roder, R. Hallmann, M. Maley, M. Davies, M. Grounds, and L. Sorokin. (1999). Expression of laminin alpha1, alpha2, alpha4, and alpha5 chains, fibronectin, and tenascin-C in skeletal muscle of dystrophic 129ReJ dy/dy mice. Exp Cell Res. *246*,165-182.

Samus, M., R. Seelige, K. Schafer, L. Sorokin, and D. Vestweber. (2018). CD99L2 deficiency inhibits leukocyte entry into the central nervous system and ameliorates neuroinflammation. J. Leukoc. Biol. *104*,787-797.

Sasaki, T., and R. Timpl. (2001). Domain IVa of laminin alpha5 chain is cell-adhesive and binds beta1 and alphaVbeta3 integrins through Arg-Gly-Asp. FEBS Lett. *509*,181-185.

Scharffetter-Kochanek, K., H. Lu, K. Norman, N. van Nood, F. Munoz, S. Grabbe, M. McArthur, I. Lorenzo, S. Kaplan, K. Ley, C.W. Smith, C.A. Montgomery, S. Rich, and A.L. Beaudet. (1998). Spontaneous skin ulceration and defective T cell function in CD18 null mice. J. Exp. Med. *188*,119-131.

Schenkel, A.R., Z. Mamdouh, X. Chen, R.M. Liebman, and W.A. Muller. (2002). CD99 plays a major role in the migration of monocytes through endothelial junctions. Nat Immunol. *3*,143-150.

Schuler, F., and L.M. Sorokin. (1995). Expression of laminin isoforms in mouse myogenic cells in vitro and in vivo. J Cell Sci. *108*,3795-3805.

Shaw, L.M., M.M. Lotz, and A.M. Mercurio. (1993). Inside-out integrin signaling in macrophages. Analysis of the role of the alpha 6A beta 1 and alpha 6B beta 1 integrin variants in laminin adhesion by cDNA expression in an alpha 6 integrin-deficient macrophage cell line. J Biol Chem. *268*,11401-11408.

Shaw, L.M., and A.M. Mercurio. (1994). Regulation of cellular interactions with laminin by integrin cytoplasmic domains: A and B structural variants of the a6b1 integrin differentially modulate the adhesive strength, morphology and migration of macrophages. Mol. Cell Biol. *5*,679-690.

Sixt, M., B. Engelhardt, F. Pausch, R. Hallmann, O. Wendler, and L.M. Sorokin. (2001a). Endothelial cell laminin isoforms, laminin 8 and 10, play decisive roles in in T-cell recruitment across the blood-brain-barrier in an experimental autoimmune encephalitis model (EAE). J Cell Biol. *153*,933-945.

Sixt, M., R. Hallmann, O. Wendler, K. Scharffetter-Kochanek, and L.M. Sorokin. (2001b). Cell adhesion and migration properties of b2-integrin negative, polymorphonuclear granulocytes (PMN) on defined extracellular matrix molecules: relevance for leukocyte extravasation. J Biol Chem. *276*,18878-18887.

Song, J., Z. Lokmic, T. Lammermann, J. Rolf, C. Wu, X. Zhang, R. Hallmann, M.J. Hannocks, N. Horn, M.A. Ruegg, A. Sonnenberg, E. Georges-Labouesse, T.H. Winkler, J.F. Kearney, S. Cardell, and L. Sorokin. (2013). Extracellular matrix of secondary lymphoid organs impacts on B-cell fate and survival. Proceedings of the National Academy of Sciences of the United States of America. *110*,E2915-2924.

Song, J., X. Zhang, K. Buscher, Y. Wang, H. Wang, J. Di Russo, L. Li, S. Lutke-Enking, A. Zarbock, A. Stadtmann, P. Striewski, B. Wirth, I. Kuzmanov, H. Wiendl, D. Schulte, D. Vestweber, and L. Sorokin. (2017). Endothelial Basement Membrane Laminin 511 Contributes to Endothelial Junctional Tightness and Thereby Inhibits Leukocyte Transmigration. Cell Rep. *18*,1256-1269.

Sorokin, L.M., F. Pausch, M. Frieser, S. Kroger, E. Ohage, and R. Deutzmann. (1997). Developmental regulation of the laminin alpha5 chain suggests a role in epithelial and endothelial cell maturation. Dev Biol. *189*,285-300.

Thomas-Ecker, S., A. Lindecke, W. Hatzmann, C. Kaltschmidt, K.S. Zanker, and T. Dittmar. (2007). Alteration in the gene expression pattern of primary monocytes after adhesion to endothelial cells. Proc. Natl. Acad. Sci. U. S. A. *104*,5539-5544.

Thyboll, J., J. Kortesmaa, R. Cao, R. Soininen, L. Wang, A. Iivanainen, L. Sorokin, M. Risling, Y. Cao, and K. Tryggvason. (2002). Deletion of the laminin alpha4 chain leads to impaired microvessel maturation. Mol Cell Biol. *22*,1194-1202.

Voisin, M.B., A. Woodfin, and S. Nourshargh. (2009). Monocytes and neutrophils exhibit both distinct and common mechanisms in penetrating the vascular basement membrane in vivo. Arterioscler Thromb Vasc Biol. *29*,1193-1199.

Wang, G.G., K.R. Calvo, M.P. Pasillas, D.B. Sykes, H. Hacker, and M.P. Kamps. (2006a). Quantitative production of macrophages or neutrophils ex vivo using conditional Hoxb8. Nat Methods. *3*,287-293.

Wang, S., M.B. Voisin, K.Y. Larbi, J. Dangerfield, C. Scheiermann, M. Tran, P.H. Maxwell, L. Sorokin, and S. Nourshargh. (2006b). Venular basement membranes contain specific matrix protein low expression regions that act as exit points for emigrating neutrophils. J Exp Med. *203*,1519-1532.

Wayner, E.A., W.G. Carter, R.S. Piotrowicz, and T.J. Kunicki. (1988). The function of multiple extracellular matrix receptors in mediating cell adhesion to extracellular matrix: preparation of monoclonal antibodies to the fibronectin receptor that specifically inhibit cell adhesion to fibronectin and react with platelet glycoproteins Ic-IIa. J Cell Biol. *107*,1881-1891.

Williams, R.L., W. Risau, H.-G. Zerwer, H. Drexler, A. Aguzzi, and E.F. Wagner. (1989). Endothelioma cells expressing the polyoma middle T oncogene induce hemangiomas by host cell recruitment. Cell. *57*,1053-1063.

Woodfin, A., M.B. Voisin, M. Beyrau, B. Colom, D. Caille, F.M. Diapouli, G.B. Nash, T. Chavakis, S.M. Albelda, G.E. Rainger, P. Meda, B.A. Imhof, and S. Nourshargh. (2011). The junctional adhesion molecule JAM-C regulates polarized transendothelial migration of neutrophils in vivo. Nat Immunol. *12*,761-769.

Woodfin, A., M.B. Voisin, and S. Nourshargh. (2007). PECAM-1: a multi-functional molecule in inflammation and vascular biology. Arterioscler. Thromb. Vasc. Biol. *27*,2514-2523.

Wu, C., F. Ivars, P. Anderson, R. Hallmann, D. Vestweber, P. Nilsson, H. Robenek, K. Tryggvason, J. Song, E. Korpos, K. Loser, S. Beissert, E. Georges-Labouesse, and L.M. Sorokin. (2009). Endothelial basement membrane laminin alpha5 selectively inhibits T lymphocyte extravasation into the brain. Nat. Med. *15*,519-527.

Zhang, X., Wang, Y., Song, J., Gerwien, H., Chusiquasana, O., Chashchina, A., Denz, C., and Sorokin, L. (2020). The endothelial basement membrane- a checkpoint for entry of pathogenic T cells into the brain. J. Exp. Med. (in press).

Zigmond, E., and S. Jung. (2013). Intestinal macrophages: well educated exceptions from the rule. Trends Immunol. *34*,162-168.

Figure 1

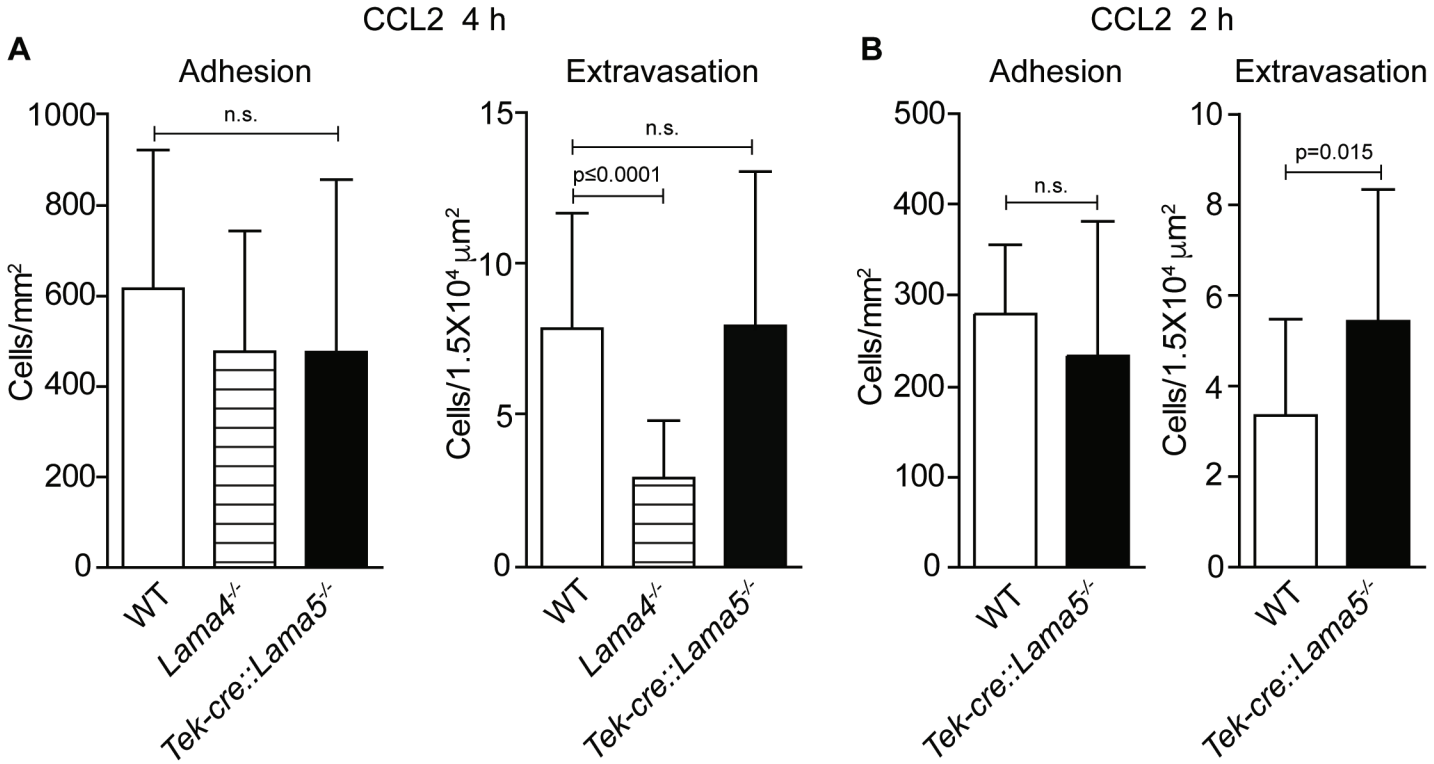
A
CCL2 4 h
Adhesion
Extravasation
Cells/mm²
Cells/1.5X10⁴ µm²
n.s.
p≤0.0001
WT
Lama4-/-
Tek-cre::Lama5-/-
B
CCL2 2 h
Adhesion
Extravasation
n.s.
p=0.015

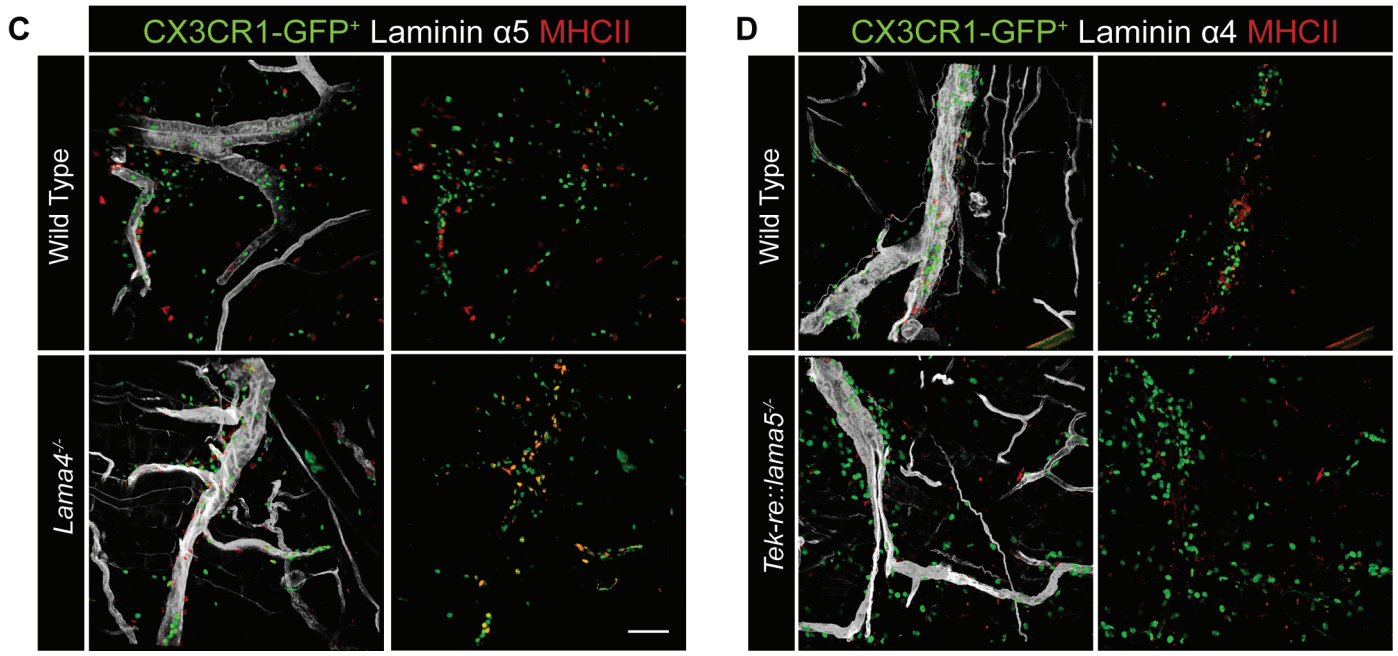
C
CX3CR1-GFP+ Laminin α5 MHCII
Wild Type
Lama4-/-
D
CX3CR1-GFP+ Laminin α4 MHCII
Wild Type
Tek-re::lama5-/-

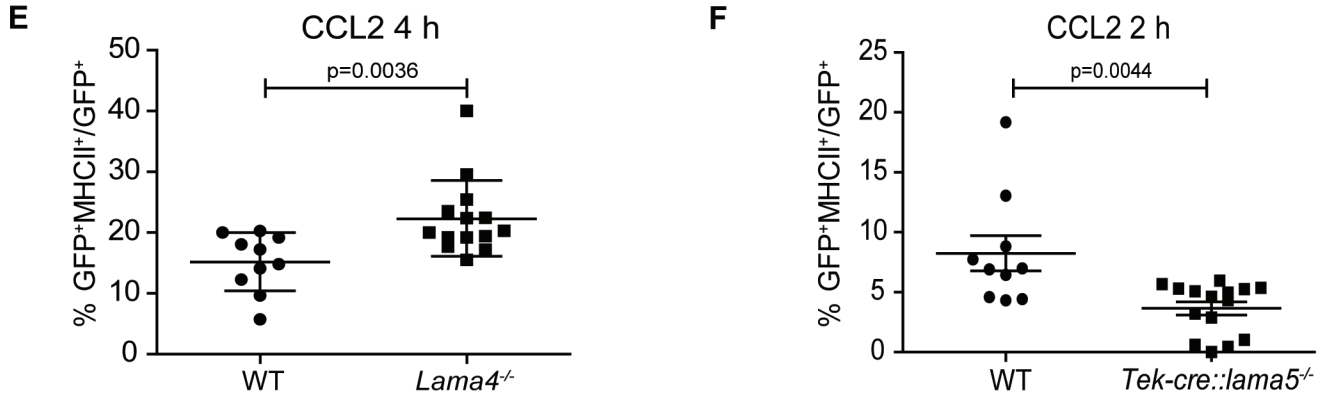
E
CCL2 4 h
p=0.0036
% GFP+MHCII+/GFP+
WT
Lama4-/-
F
CCL2 2 h
p=0.0044
% GFP+MHCII+/GFP+
WT
Tek-cre::lama5-/-

Figure 2

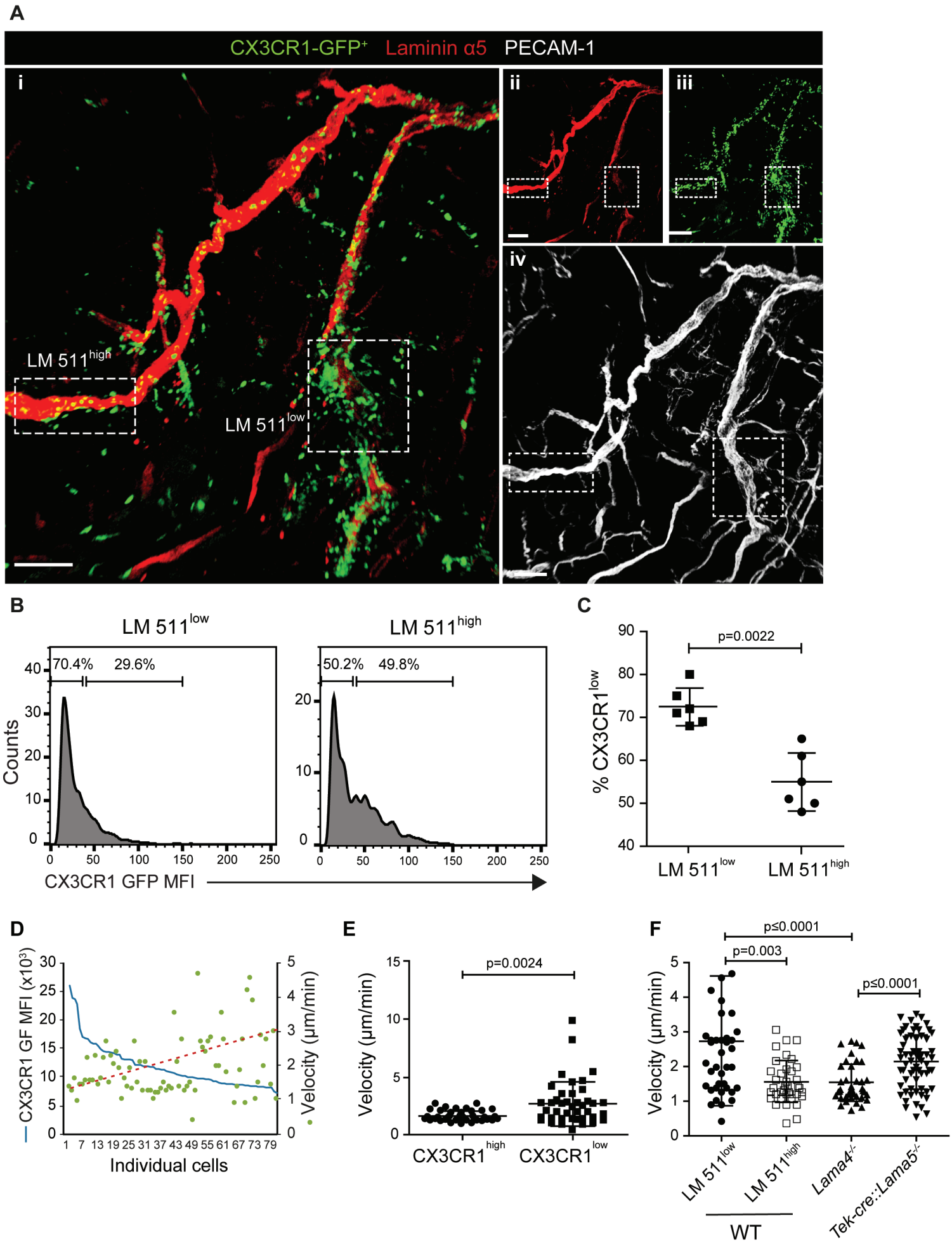
A
CX3CR1-GFP+ Laminin α5 PECAM-1
i
ii
iii
iv
LM 511high
LM 511low
B
LM 511low
LM 511high
70.4%
29.6%
50.2%
49.8%
Counts
CX3CR1 GFP MFI
C
p=0.0022
% CX3CR1low
LM 511low
LM 511high
D
CX3CR1 GF MFI (x10³)
Velocity (µm/min)
Individual cells
E
p=0.0024
Velocity (µm/min)
CX3CR1high
CX3CR1low
F
p≤0.0001
p=0.003
p≤0.0001
Velocity (µm/min)
LM 511low
LM 511high
Lama4-/-
Tek-cre::Lama5-/-
WT

Figure 3

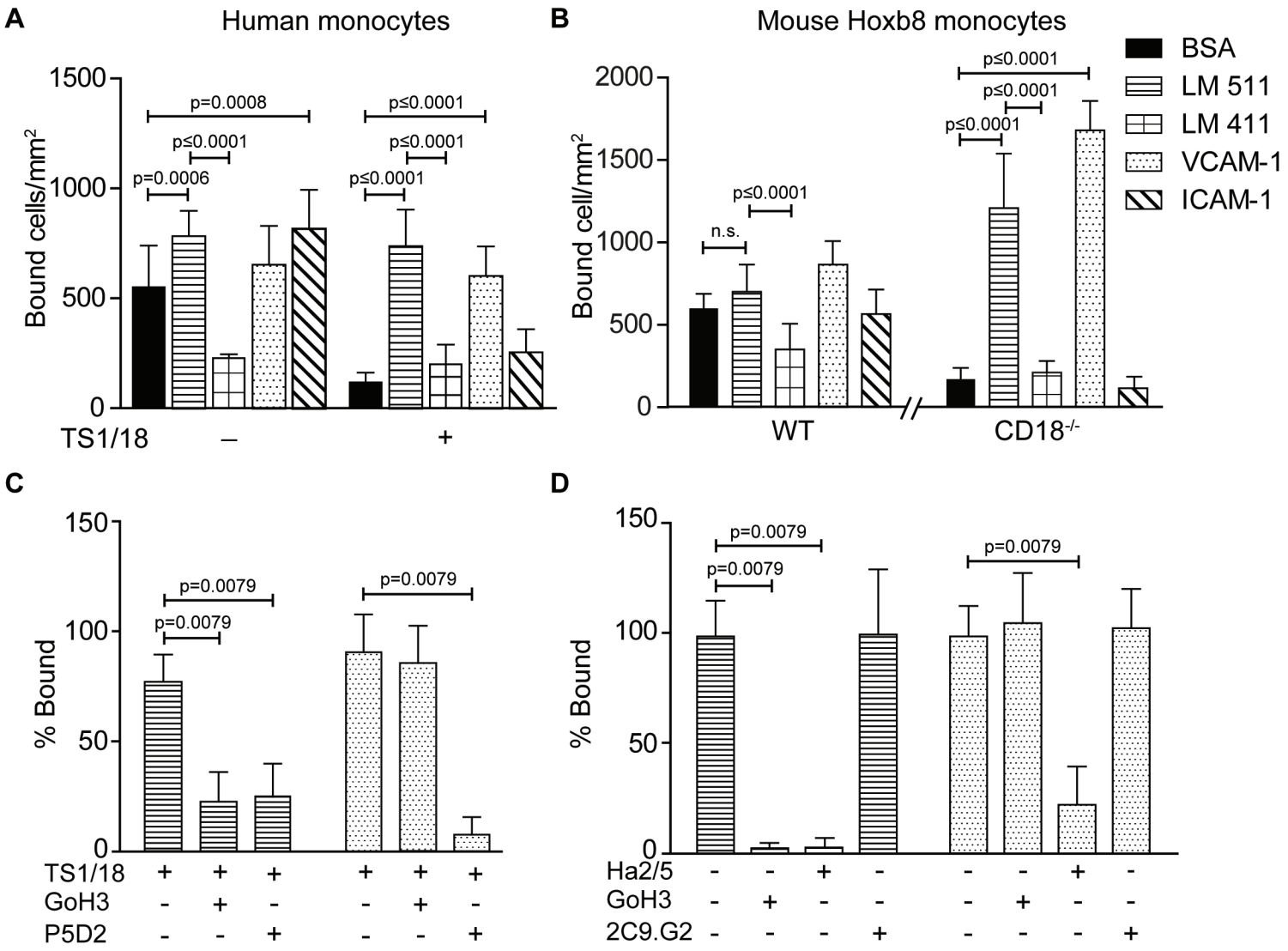
A
Human monocytes
Bound cells/mm²
1500
1000
500
0
p=0.0008
p≤0.0001
p=0.0006
p≤0.0001
p≤0.0001
p≤0.0001
TS1/18
–
+
B
Mouse Hoxb8 monocytes
Bound cell/mm²
2000
1500
1000
500
0
n.s.
p≤0.0001
p≤0.0001
p≤0.0001
p≤0.0001
WT
CD18-/-
BSA
LM 511
LM 411
VCAM-1
ICAM-1
C
% Bound
150
100
50
0
p=0.0079
p=0.0079
p=0.0079
TS1/18 + + + + + +
GoH3 - + - - + -
P5D2 - - + - - +
D
% Bound
150
100
50
0
p=0.0079
p=0.0079
p=0.0079
Ha2/5 - - + - - - + -
GoH3 - + - - - + - -
2C9.G2 - - - + - - - +

Figure 4

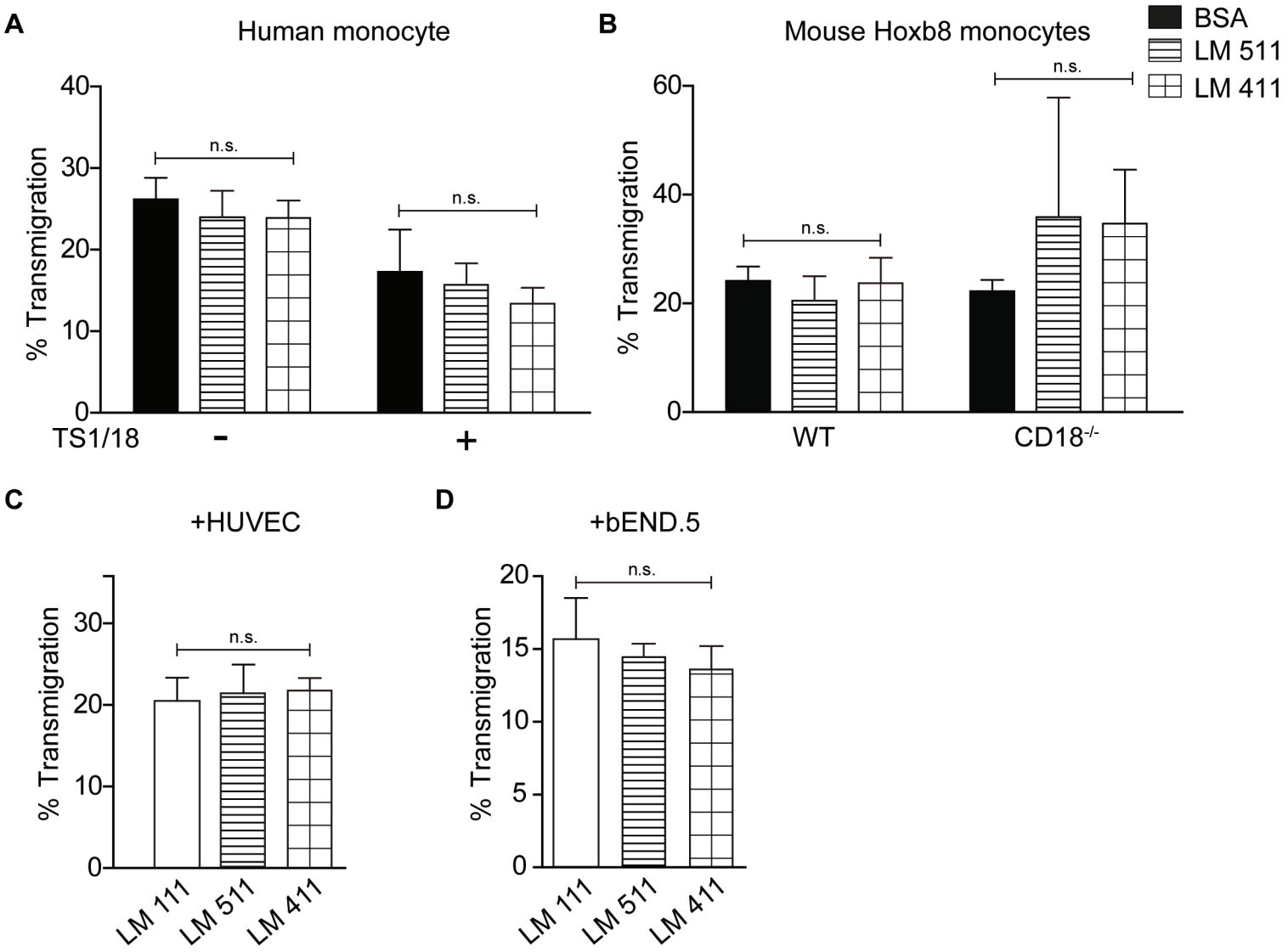
A
Human monocyte
% Transmigration
40
30
20
10
0
n.s.
n.s.
TS1/18
-
+
B
Mouse Hoxb8 monocytes
BSA
LM 511
LM 411
% Transmigration
60
40
20
0
n.s.
n.s.
WT
CD18-/-
C
+HUVEC
% Transmigration
30
20
10
0
n.s.
LM 111
LM 511
LM 411
D
+bEND.5
% Transmigration
20
15
10
5
0
n.s.
LM 111
LM 511
LM 411

Figure 5

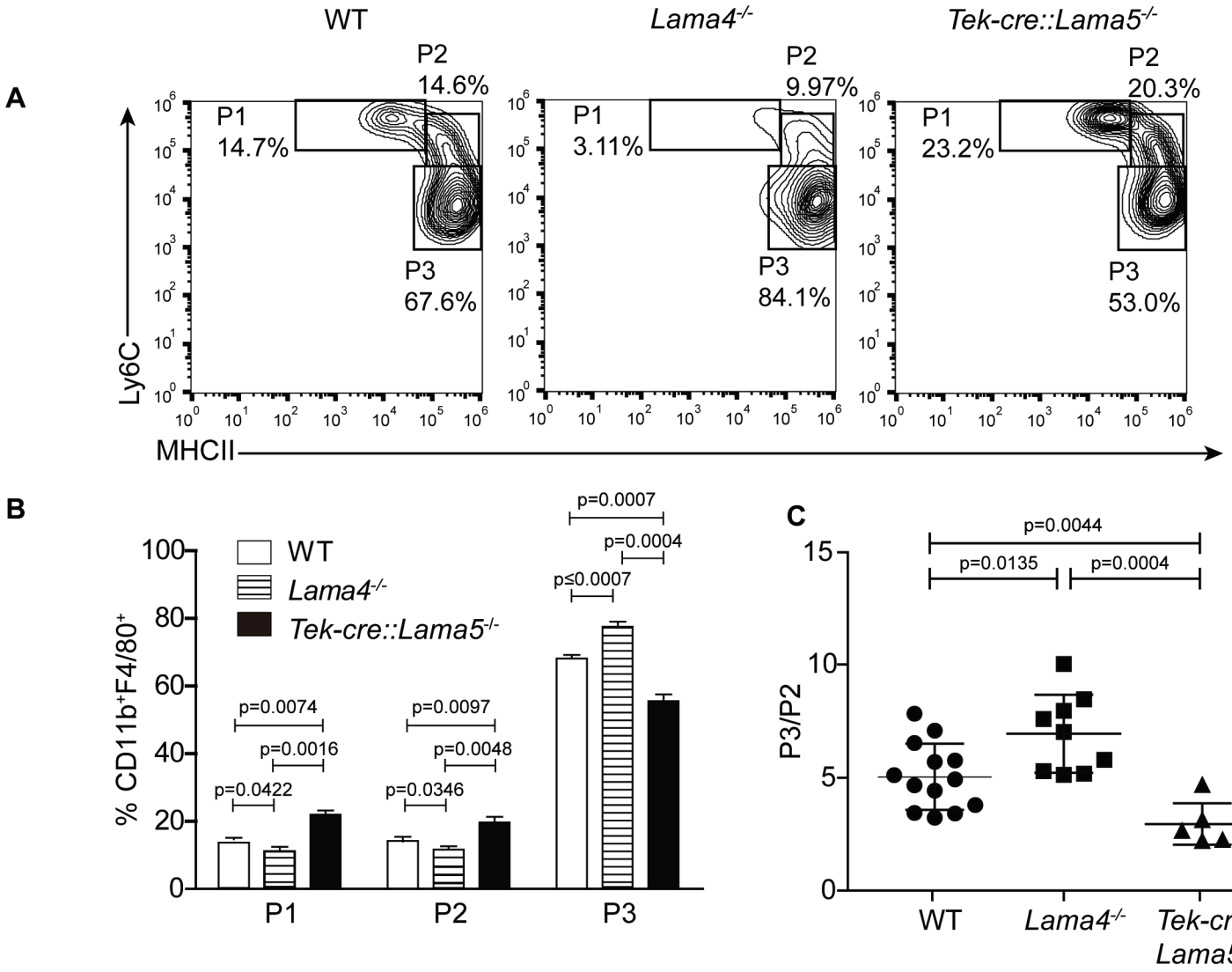
A
WT
Lama4-/-
Tek-cre::Lama5-/-
P1
14.7%
P2
14.6%
P3
67.6%
P1
3.11%
P2
9.97%
P3
84.1%
P1
23.2%
P2
20.3%
P3
53.0%
Ly6C
MHCII
B
WT
Lama4-/-
Tek-cre::Lama5-/-
% CD11b+F4/80+
p=0.0422
p=0.0016
p=0.0074
p=0.0346
p=0.0048
p=0.0097
p≤0.0007
p=0.0004
p=0.0007
P1
P2
P3
C
p=0.0044
p=0.0135
p=0.0004
P3/P2
WT
Lama4-/-
Tek-cre::
Lama5-/-

Figure 6

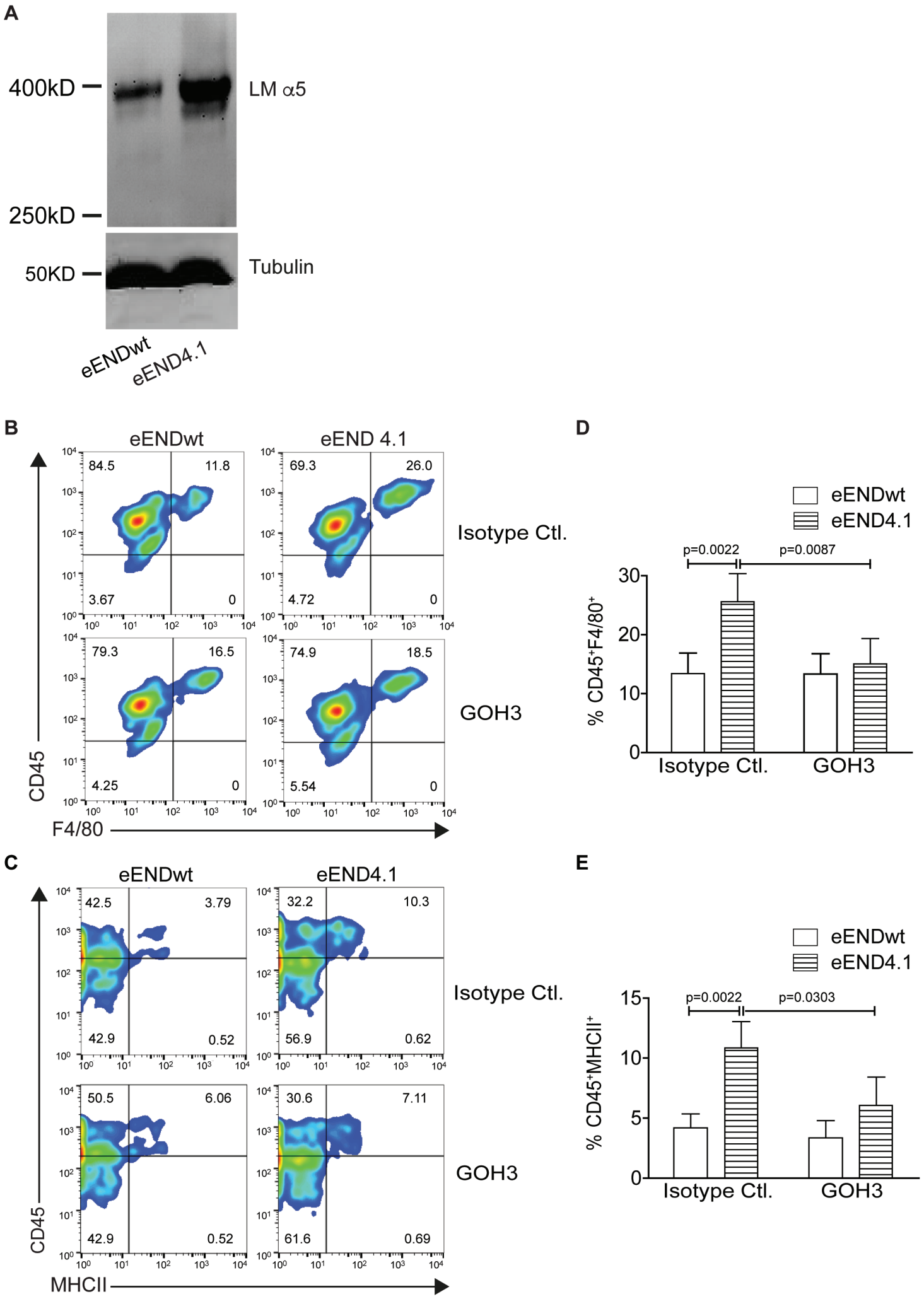
A
400kD
250kD
LM α5
50KD
Tubulin
eENDwt
eEND4.1
B
eENDwt
eEND 4.1
84.5
11.8
3.67
0
69.3
26.0
4.72
0
Isotype Ctl.
79.3
16.5
4.25
0
74.9
18.5
5.54
0
GOH3
CD45
F4/80
C
eENDwt
eEND4.1
42.5
3.79
42.9
0.52
32.2
10.3
56.9
0.62
Isotype Ctl.
50.5
6.06
42.9
0.52
30.6
7.11
61.6
0.69
GOH3
CD45
MHCII
D
eENDwt
eEND4.1
p=0.0022
p=0.0087
% CD45+F4/80+
Isotype Ctl.
GOH3
E
eENDwt
eEND4.1
p=0.0022
p=0.0303
% CD45+MHCII+
Isotype Ctl.
GOH3

Figure 7

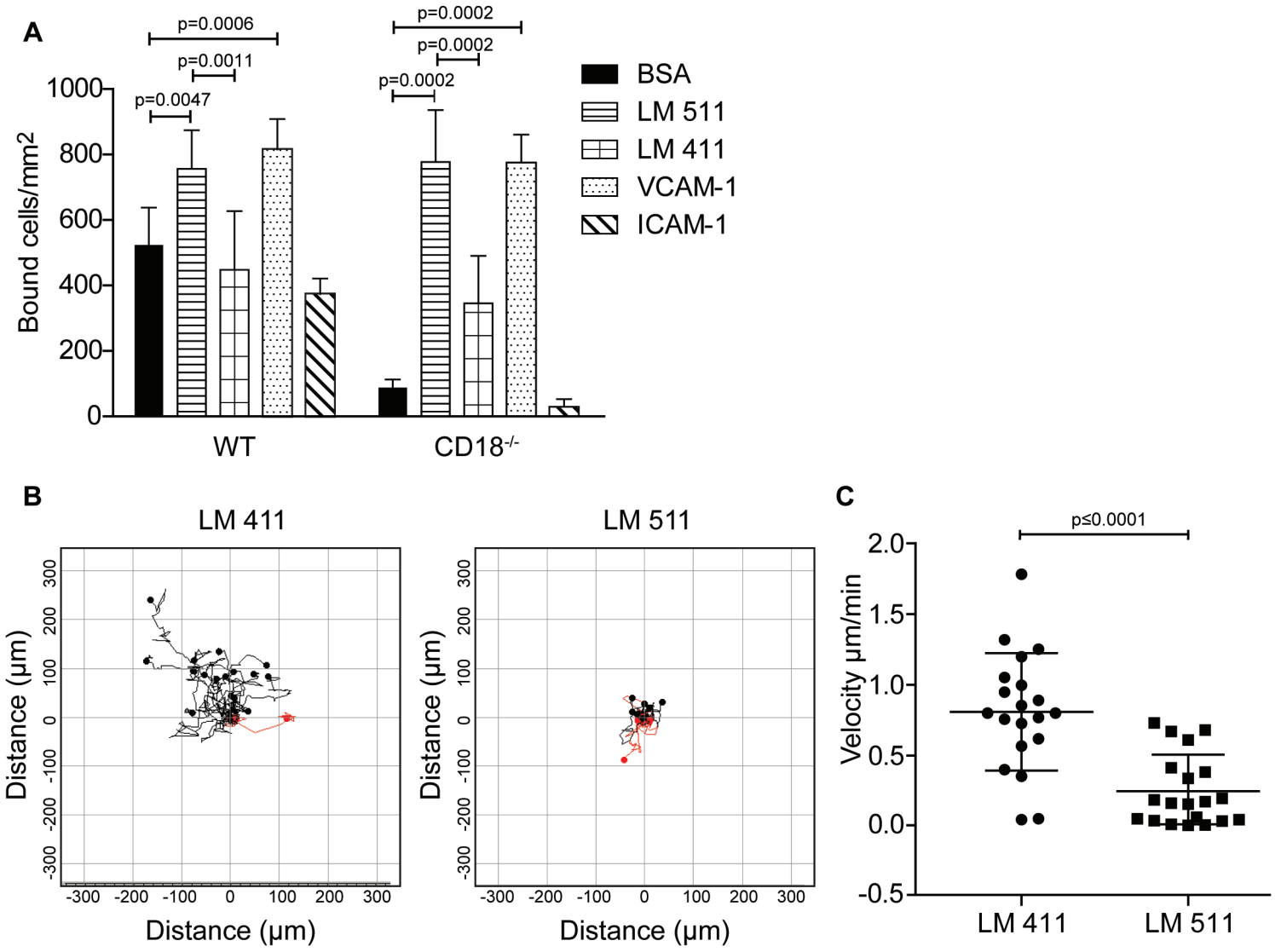
A
p=0.0006
p=0.0011
p=0.0047
p=0.0002
p=0.0002
p=0.0002
Bound cells/mm2
1000
800
600
400
200
0
WT
CD18-/-
BSA
LM 511
LM 411
VCAM-1
ICAM-1
B
LM 411
LM 511
Distance (µm)
Distance (µm)
-300 -200 -100 0 100 200 300
C
p≤0.0001
Velocity µm/min
2.0
1.5
1.0
0.5
0.0
-0.5
LM 411
LM 511

Supplemental Information

Fig. S1 Images taken from movies of CX3CR1-GFP^{+} cells extravasating across postcapillary venules of the cremaster muscle of WT, *Lama4*$^{-/-}$ and *Tek-cre::Lama5*$^{-/-}$ mice; related to Figures 1 and 2. Boxed areas are 75 μm from either side of the postcapillary venule for a length of 100 μm, that were used to quantify extravasated CX3CR1-GFP^{+} cells; scale bars = 50μm

Fig. S2 Representative flow cytometry for integrin subunits; related to Figures 2 and 3. (A) Primary human monocytes, (B) mouse monocyte-like Hoxb8 cells derived from CD18$^{-/-}$ mice and their WT littermates, and (C) WT and CD18$^{-/-}$ bone marrow derived macrophages (C).

Fig. S3 Dot blots for the expression of laminin α4 and laminin α5 polypeptides in mouse and human monocytic cells and sera; related to Figure 4. Cell lysates from untreated and LPS treated mouse Hoxb8 precursors and monocytes, bone marrow derived macrophages (BMDM), and sera from WT and *Lama4*$^{-/-}$ mice were analysed by dot-blot using rabbit anti-mouse laminin α4 antibody (377) (Ringelmann et al., 1999), pre-immune serum and secondary antibody only. (B) Mouse Hoxb8 monocytes and BMDM were analysed using purified rabbit anti-mouse laminin α5 (405) (Ringelmann et al., 1999). (C) Human monocyte lysates and sera were blotted and stained with mouse anti-human laminin α4 (3D12) (Korpos et al., 2013) or only 2nd antibody. (D) Human monocyte lysates were analysed using mouse anti-human laminin α5 (6A11) (Korpos et al., 2013). Dots of 5μg total protein or serum were analysed; dashed lines mark area of drops.

Fig. S4 Gating strategy employed for identification of P1, P2 and P2 differentiating macrophage populations in the colon lamina propria; related to Figure 5. Modified from Bain et al., (2014)(Bain et al., 2014). Cell aggregates and dead cells were excluded by FSC and viability dye staining, respectively. Total leukocytes were selected by CD45 expression; Ly6G^{+} neutrophils and Siglec-F^{+} eosinophils were then gated out from CD45^{+} population. To obtain F4/80^{+}CD11b^{+} cells, the CD11c^{high}F4/80^{low} mucosal dendritic cells (DC), were gated out. Based on Ly6C and MHCII levels, the F4/80^{+}CD11b^{+} cells were further divided to P1 (Ly6C^{high}MHCII^{low}), P2 (Ly6C^{mid}MHCII^{mid}) and P3 (Ly6C^{low}MHCII^{high}) populations. (B) Representative flow cytometry of early extravasating P1 (Ly6C^{hi}MHCII^{low}) plus P2 (Ly6C^{mid}MHCII^{mid}) populations, and mature P3 macrophages (Ly6C^{low}MHCII^{hi}) in isolated colonic lamina propria cells from P21 WT, *Lama4*$^{-/-}$ and *Tek-cre::Lama5*$^{-/-}$ mice; and (C) corresponding quantification of the data. (D) Ratios of P3 /P2+P1 cells. Data are means ± SD from 4 experiments performed with 23 WT, 9 *Lama4*$^{-/-}$ and 7 *Tek-cre::Lama5*$^{-/-}$ mice . Significance was calculated using the Mann-Whitney-Test, since not all data passed the normality test by D`Adostino & Pearson; exact *p*-values are indicated in the graph.

Fig. S5 Characterization of eEND4.1 and eENDwt endothelioma cell lines; related to Figure 6. Endotheliomas were derived from *Lama4*$^{-/-}$ embryos (eEND4.1) and their WT littermates (eENDwt) and flow cytometry of splenic monocytes employed in experiments shown in Fig. 6 of the main text. (A) Full Western blot with secondary antibody control shown in Fig. 6A. Representative flow cytometry of sorted splenic monocytes employed Fig. 6B (B) and Fig. 6C (C) before and after 16 h incubation in the absence of endothelial cells.

Figure S1

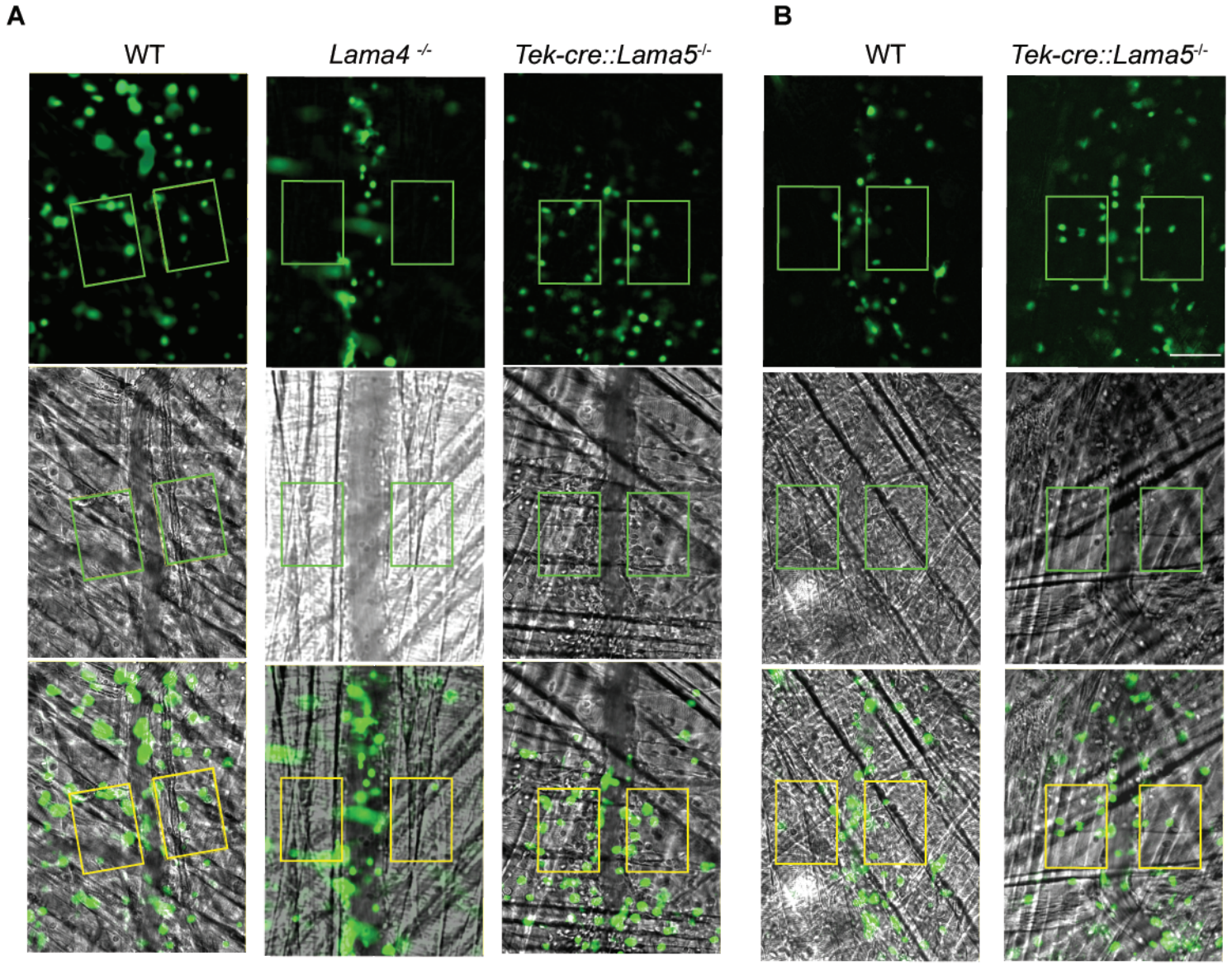

Figure S2

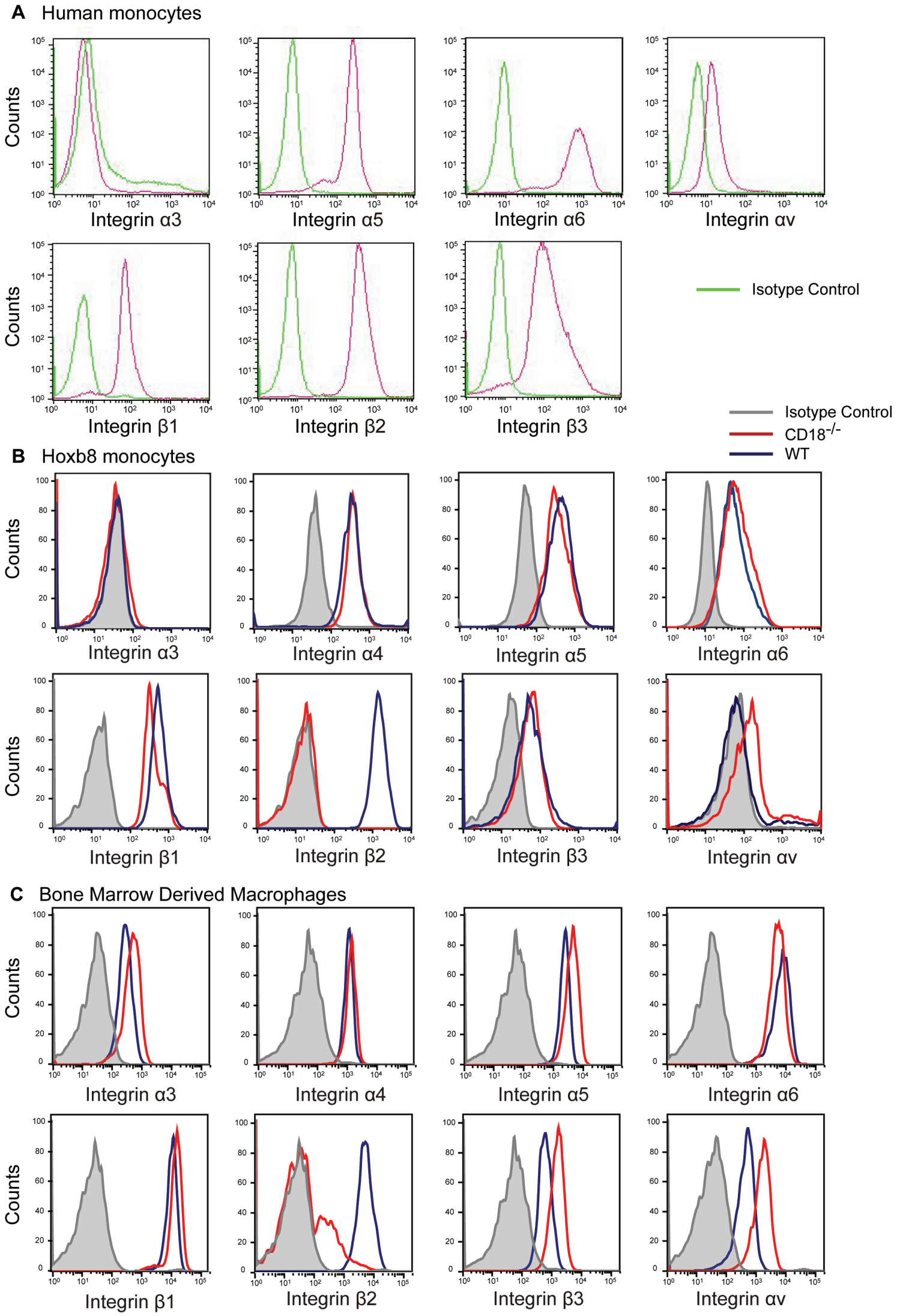
A Human monocytes
Counts
Integrin α3
Integrin α5
Integrin α6
Integrin αv
Integrin β1
Integrin β2
Integrin β3
Isotype Control
Isotype Control
CD18-/-
WT
B Hoxb8 monocytes
Integrin α3
Integrin α4
Integrin α5
Integrin α6
Integrin β1
Integrin β2
Integrin β3
Integrin αv
C Bone Marrow Derived Macrophages
Integrin α3
Integrin α4
Integrin α5
Integrin α6
Integrin β1
Integrin β2
Integrin β3
Integrin αv

Figure S3

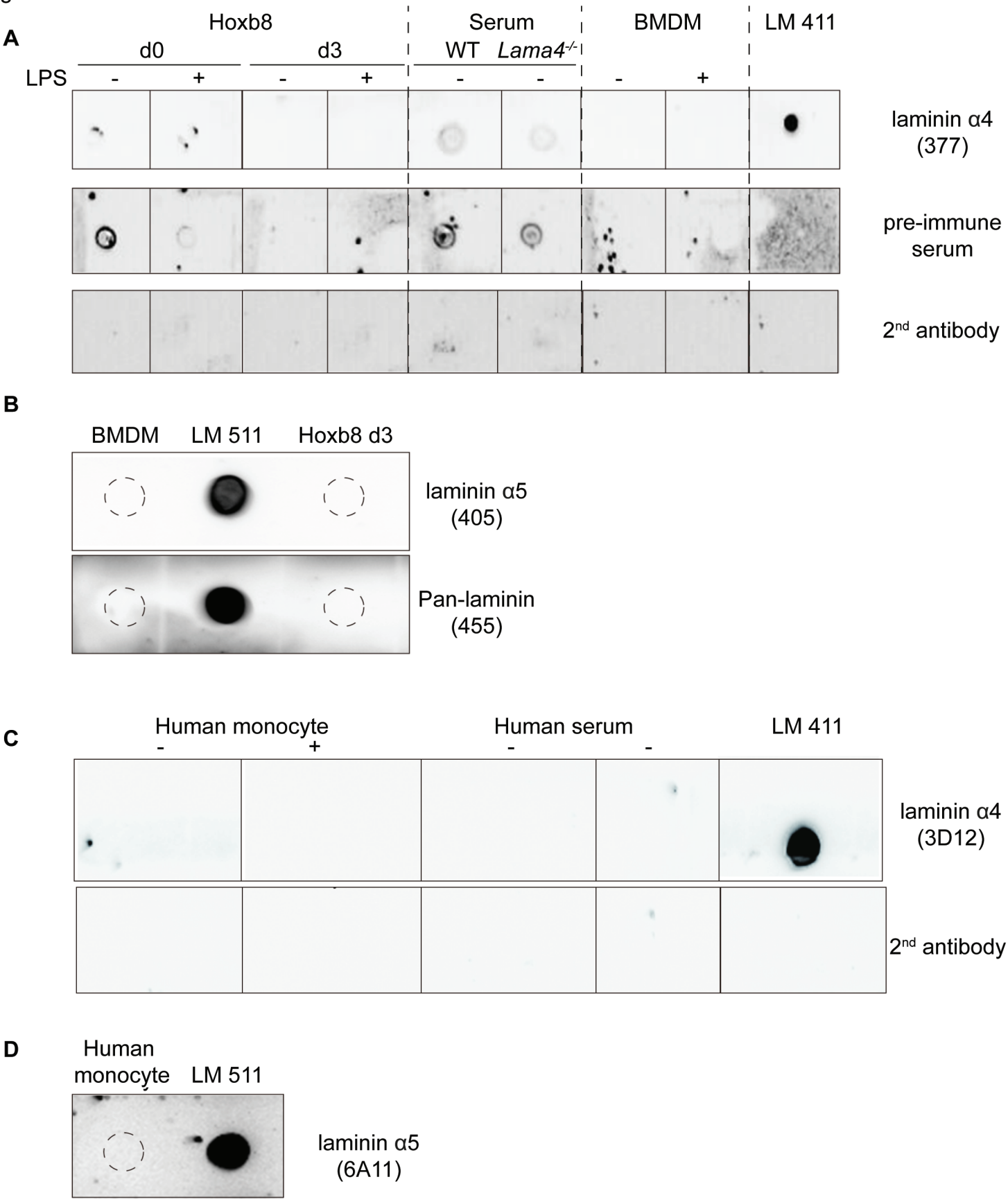
A
Hoxb8
d0
d3
Serum
WT
Lama4-/-
BMDM
LM 411
LPS
-
+
-
+
-
-
-
+
laminin α4 (377)
pre-immune serum
2nd antibody
B
BMDM
LM 511
Hoxb8 d3
laminin α5 (405)
Pan-laminin (455)
C
Human monocyte
-
+
Human serum
-
-
LM 411
laminin α4 (3D12)
2nd antibody
D
Human monocyte
LM 511
laminin α5 (6A11)

Figure S4

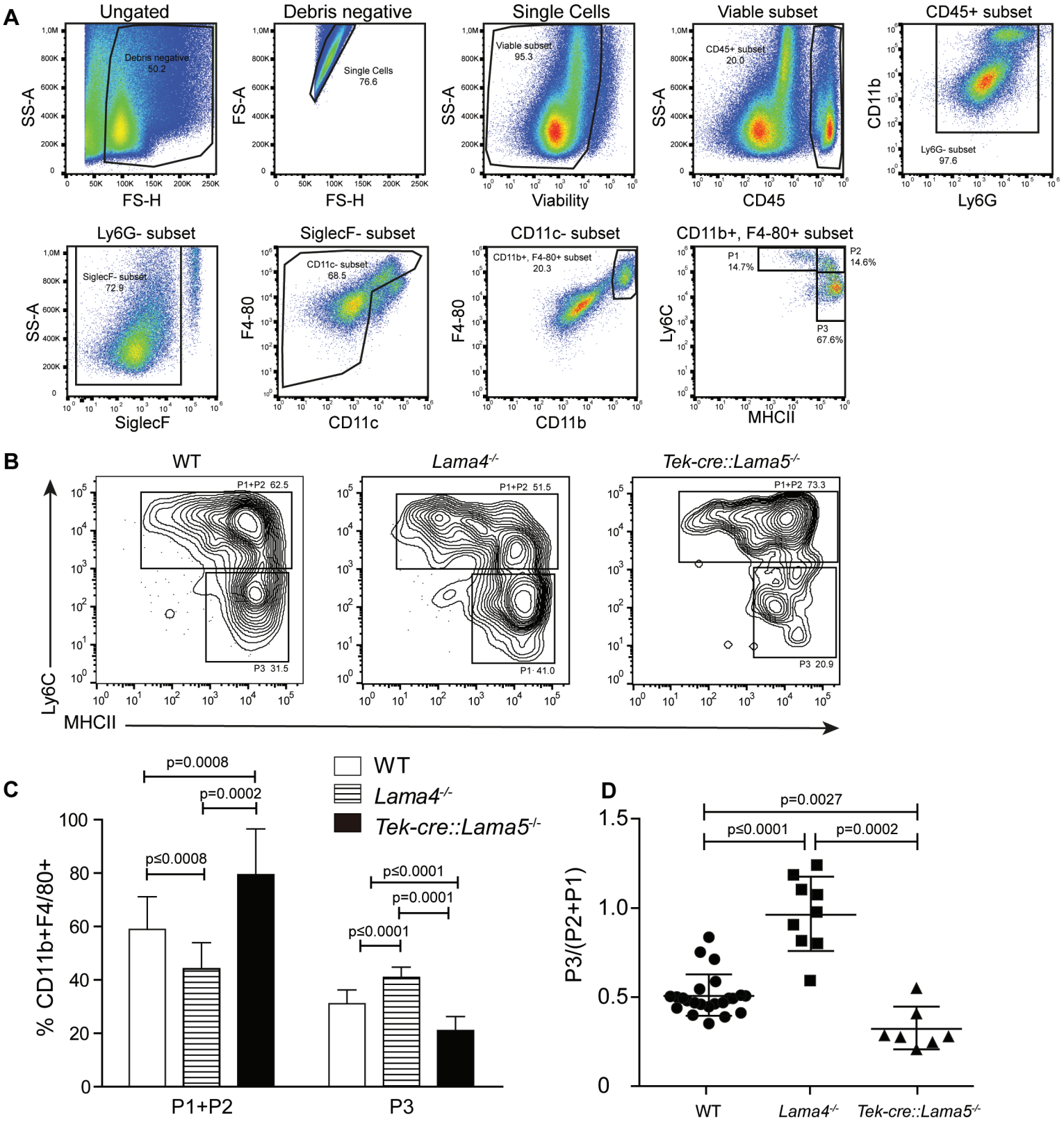
A
Ungated
Debris negative
50.2
SS-A
FS-H
Debris negative
Single Cells
76.6
FS-A
FS-H
Single Cells
Viable subset
95.3
SS-A
Viability
Viable subset
CD45+ subset
20.0
SS-A
CD45
CD45+ subset
Ly6G- subset
97.6
CD11b
Ly6G
Ly6G- subset
SiglecF- subset
72.9
SS-A
SiglecF
SiglecF- subset
CD11c- subset
68.5
F4-80
CD11c
CD11c- subset
CD11b+, F4-80+ subset
20.3
F4-80
CD11b
CD11b+, F4-80+ subset
P1
14.7%
P2
14.6%
P3
67.6%
Ly6C
MHCII
B
WT
Lama4-/-
Tek-cre::Lama5-/-
P1+P2 62.5
P3 31.5
P1+P2 51.5
P1 41.0
P1+P2 73.3
P3 20.9
Ly6C
MHCII
C
WT
Lama4-/-
Tek-cre::Lama5-/-
p=0.0008
p=0.0002
p≤0.0008
p≤0.0001
p=0.0001
p≤0.0001
% CD11b+F4/80+
P1+P2
P3
D
p=0.0027
p≤0.0001
p=0.0002
P3/(P2+P1)
WT
Lama4-/-
Tek-cre::Lama5-/-

Figure S5

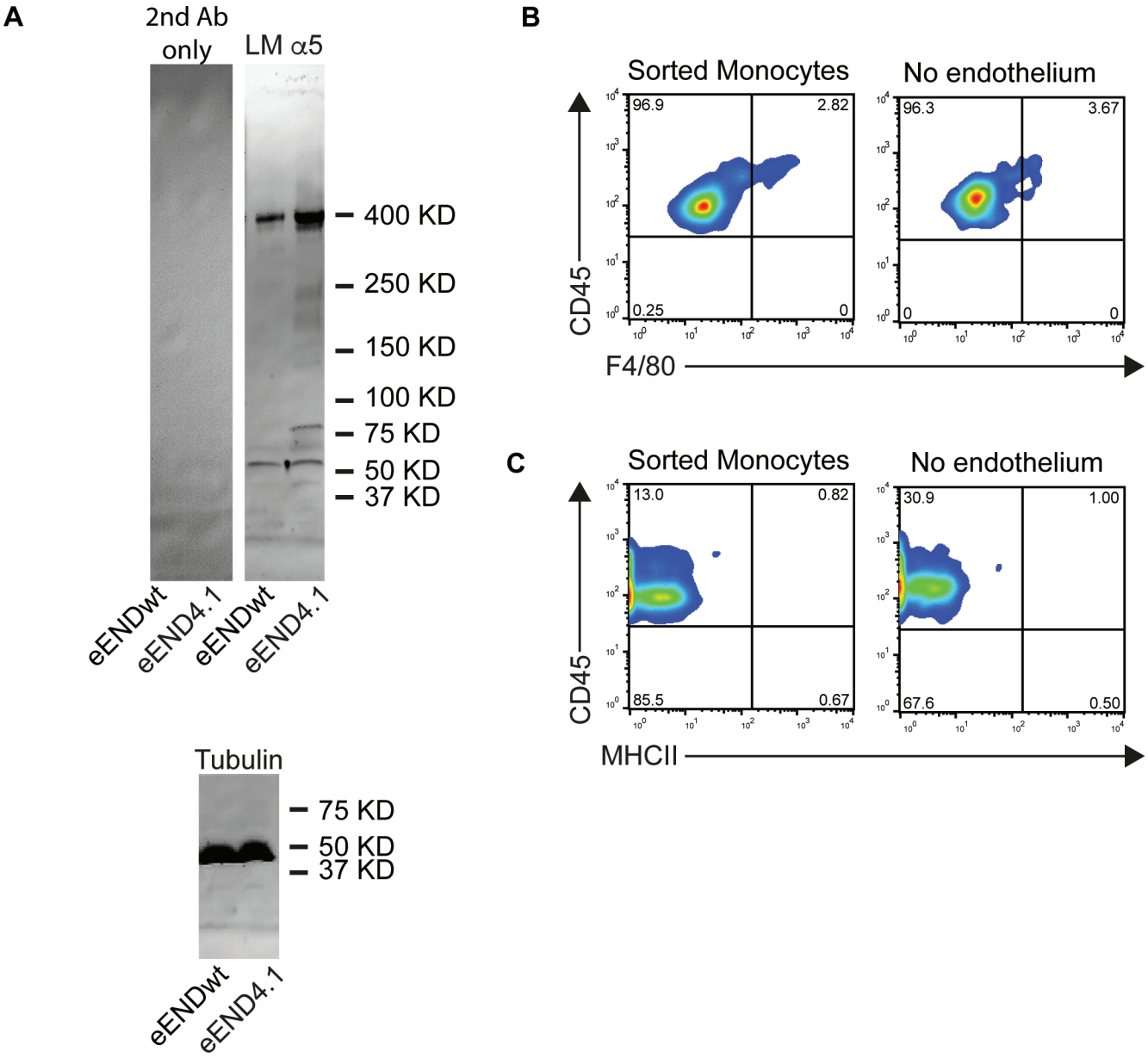
A
2nd Ab only
LM α5
400 KD
250 KD
150 KD
100 KD
75 KD
50 KD
37 KD
eENDwt
eEND4.1
eENDwt
eEND4.1
Tubulin
75 KD
50 KD
37 KD
eENDwt
eEND4.1
B
Sorted Monocytes
No endothelium
96.9
2.82
0.25
0
96.3
3.67
0
0
CD45
F4/80
C
Sorted Monocytes
No endothelium
13.0
0.82
85.5
0.67
30.9
1.00
67.6
0.50
CD45
MHCII